Radiative seesaw corrections and charged-lepton decays in a model with soft flavour violation

E.H. Aeikens,[a] **P.M. Ferreira,**[b,c] **W. Grimus,**[a] **D. Jurčiukonis**[d] **and L. Lavoura**[e]

[a]*University of Vienna, Faculty of Physics,*
Boltzmanngasse 5, A-1090 Wien, Austria

[b]*Instituto Superior de Engenharia de Lisboa — ISEL,*
1959-007 Lisboa, Portugal

[c]*Centro de Física Teórica e Computacional, Faculdade de Ciências, Universidade de Lisboa,*
Av. Prof. Gama Pinto 2, 1649-003 Lisboa, Portugal

[d]*Vilnius University, Institute of Theoretical Physics and Astronomy,*
Saulėtekio ave. 3, Vilnius 10257, Lithuania

[e]*Universidade de Lisboa, Instituto Superior Técnico, CFTP,*
Av. Rovisco Pais 1, 1049-001 Lisboa, Portugal

E-mail: elke.aeikens@univie.ac.at, pmmferreira@fc.ul.pt,
walter.grimus@univie.ac.at, darius.jurciukonis@tfai.vu.lt,
balio@cftp.tecnico.ulisboa.pt

ABSTRACT: We consider the one-loop radiative corrections to the light-neutrino mass matrix and their consequences for the predicted branching ratios of the five lepton-flavour-violating decays $\ell_1^- \to \ell_2^- \ell_3^+ \ell_3^-$ in a two-Higgs-doublet model furnished with the type-I seesaw mechanism and *soft* lepton-flavour violation. We find that the radiative corrections are very significant; they may alter the predicted branching ratios by several orders of magnitude and, in particular, they may help explain why BR $\left(\mu^- \to e^- e^+ e^-\right)$ is strongly suppressed relative to the branching ratios of the decays of the τ^-. We conclude that, in any serious numerical assessment of the predictions of this model, it is absolutely necessary to take into account the one-loop radiative corrections to the light-neutrino mass matrix.

Contents

1 Introduction

The existence of neutrino oscillations is now firmly established — see [1–4] and references therein. Therefore, the violation of the family lepton numbers L_ℓ ($\ell = e, \mu, \tau$) is firmly established as well. However, no violation of the L_ℓ but for neutrino oscillations has been hitherto detected. In this context, the flavour-violating charged-lepton decays are of particular importance, because it is expected that in the near future the experimental bounds on the branching ratios (BRs) of those decays will be improved substantially [5–9] (see also section 2 of [10]). It is thus important to address those decays in specific models for the neutrino masses and lepton mixings — and the more so since, when one incorporates neutrino masses and lepton mixings in the Standard Model (SM), those BRs are so small that the decays are in practice invisible [11–14].

In this letter we discuss the model put forward in [15, 16]. This is in general *a multi-Higgs-doublet extension of the SM* (for reviews see [17, 18]), but we confine ourselves to just two Higgs doublets. The model has *three right-handed neutrino singlets $\nu_{\ell R}$ that enable the seesaw mechanism* [19–23]. The lepton Yukawa couplings are

$$\mathcal{L}_{\text{Yukawa}} = -\sum_{\ell_1,\,\ell_2 = e,\mu,\tau} \left[\left(\varphi_1^-,\, \varphi_1^{0*} \right) \bar{\ell}_{1R} \left(Y_1 \right)_{\ell_1 \ell_2} + \left(\varphi_1^0,\, -\varphi_1^+ \right) \bar{\nu}_{\ell_1 R} \left(Z_1 \right)_{\ell_1 \ell_2} \right.$$
$$\left. + \left(\varphi_2^-,\, \varphi_2^{0*} \right) \bar{\ell}_{1R} \left(Y_2 \right)_{\ell_1 \ell_2} + \left(\varphi_2^0,\, -\varphi_2^+ \right) \bar{\nu}_{\ell_1 R} \left(Z_2 \right)_{\ell_1 \ell_2} \right] \begin{pmatrix} \nu_{\ell_2 L} \\ \ell_{2L} \end{pmatrix} + \text{H.c.}, \quad (1.1)$$

where $Y_{1,2}$ and $Z_{1,2}$ are Yukawa-coupling matrices. A crucial feature of the model is *the imposition of three global* $\text{U}(1)_\ell$ *symmetries associated with the family lepton numbers L_ℓ*; those symmetries force $Y_{1,2}$ and $Z_{1,2}$ to be diagonal. (The lepton numbers of the two Higgs doublets are zero.) Without loss of generality, in this letter we use the 'Higgs basis', wherein only the first doublet has a nonzero vacuum expectation value $v \left/ \sqrt{2} \right.$, where $v \simeq 246\,\text{GeV}$ is real and positive, in its neutral component φ_1^0. This allows us to rewrite (1.1) as

$$\mathcal{L}_{\text{Yukawa}} = -\sum_{\ell = e,\mu,\tau} \left[\left(\varphi_1^-,\, \varphi_1^{0*} \right) \bar{\ell}_R \frac{\sqrt{2} m_\ell}{v} + \left(\varphi_1^0,\, -\varphi_1^+ \right) \bar{\nu}_{\ell R}\, d_\ell \right.$$
$$\left. + \left(\varphi_2^-,\, \varphi_2^{0*} \right) \bar{\ell}_R\, \gamma_\ell + \left(\varphi_2^0,\, -\varphi_2^+ \right) \bar{\nu}_{\ell R}\, \delta_\ell \right] \begin{pmatrix} \nu_{\ell L} \\ \ell_L \end{pmatrix} + \text{H.c.}, \quad (1.2)$$

where the m_ℓ are the (real and positive) charged-lepton masses and d_ℓ, γ_ℓ, and δ_ℓ are dimensionless and, in general, complex Yukawa coupling constants.

In our model *the source of lepton-flavour violation lies exclusively in the Majorana mass matrix M_R of the right-handed neutrinos*. In other words, the only lepton-flavour-violating (LFV) terms in the Lagrangian are in

$$\mathcal{L}_{\nu_R\,\text{mass}} = -\frac{1}{2} \sum_{\ell_1, \ell_2 = e,\mu,\tau} (M_R)_{\ell_1 \ell_2}\, \bar{\nu}_{\ell_1 R}\, C\, \bar{\nu}_{\ell_2 R}^T + \text{H.c.}, \quad (1.3)$$

where $(M_R)_{\ell_1 \ell_2} = (M_R)_{\ell_2 \ell_1}$ are coefficients with mass dimension and C is the charge-conjugation matrix in Dirac space. The salient feature of this model is the *soft* nature of the breaking of the L_ℓ [15, 24] by $\mathcal{L}_{\nu_R\,\text{mass}}$. Soft-breaking of a symmetry means that the symmetry is preserved by dimension-four terms in the Lagrangian, *viz.* the Yukawa couplings (1.2), but it is broken by terms with mass dimension smaller than four, *viz.* the Majorana masses (1.3). In our model, the softness of the breaking ensures that the one-loop amplitudes of LFV charged-lepton decays are finite, as was explicitly demonstrated by two of us in [15].[1]

---

[1]This mechanism for suppressing undesirable flavour-changing neutral currents has no counterpart in the quark sector. Since we do not want to set to zero any of the Yukawa couplings in (1.2), the two Higgs doublets cannot transform non-trivially under any global symmetry. Therefore, at this stage, we can only resort to finetuning in the quark sector. In the present letter we shall not address this issue any further.

Let $S_a^{\pm}$ ($a = 1, 2$) and S_b^0 ($b = 1, 2, 3, 4$) denote, respectively, the charged-scalar and the (real) neutral-scalar mass eigenfields of our two-Higgs-doublet model (2HDM). By definition, $S_1^+ \equiv G^+$ and $S_1^0 \equiv G^0$ are, respectively, the charged and the neutral Goldstone bosons. Again by definition, $S_2^0 \equiv H$ is the physical scalar with mass $m_H \simeq 125\,\text{GeV}$ that has been observed at the LHC. Let M_3 and M_4 denote the masses of S_3^0 and S_4^0, respectively.

It is an outstanding feature of our model that the amplitudes for the radiative decays $\ell_1^{\pm} \to \ell_2^{\pm}\gamma$ and $Z^0 \to \ell_1^+ \ell_2^-$ ($\ell_1 \neq \ell_2$) are suppressed by m_R^{-2}, where m_R is the seesaw scale [15]; one can estimate that for $m_R \gtrsim 10^3\,\text{TeV}$ these decays are invisible, in the foreseeable future, in the context of our model [16] (another model with this feature is discussed in [25]). The same suppression occurs when the gauge bosons are off-mass shell, *viz.* in the one-loop diagrams for the LFV decays $\mu^- \to e^- e^+ e^-$ and $\tau^- \to \ell_2^- \ell_3^+ \ell_3^-$ ($\ell_2, \ell_3 = e, \mu$) [15] where those decays are mediated by either a virtual γ or a virtual Z^0.[2] On the other hand, those five decays also have one-loop amplitudes mediated by neutral-scalar exchange, and these amplitudes are *unsuppressed* when $m_R \to \infty$ [15]. It is the purpose of this letter to present a theoretical and numerical study of these three-body decays while *taking into account the radiative corrections to the seesaw mass matrix of the light neutrinos* [26]. The latter point is new when compared to [16], and it is important because of two reasons:

- For M_3 or M_4 larger than $4\pi v \sim 3\,\text{TeV}$, and provided the Yukawa couplings d_ℓ and $\delta_{\ell'}$ are of similar order of magnitude, the radiative corrections to the neutrino mass matrix are dominant;[3] they are non-negligible even for values of $M_{3,4}$ much lower than that.

- The branching ratios $\text{BR}\left(\ell_1^- \to \ell_2^- \ell_3^+ \ell_3^-\right)$ depend on the mass matrix M_R [15, 16] — see section 2. Information on M_R is not directly available but has to be extracted from the mass matrix of the light neutrinos. The latter matrix may be assembled from the light-neutrino masses and from the lepton mixing obtained from fits to the neutrino oscillation data. Therefore, the radiative corrections to the mass matrix of the light neutrinos will influence the extraction of M_R. Indeed, they may alter the branching ratios drastically, as we shall see later.

Henceforth, for the sake of brevity, the acronym 'BR' will always refer to the branching ratios of the five decays $\ell_1^- \to \ell_2^- \ell_3^+ \ell_3^-$; the same will apply to the phrase 'decay rate'.

Although in this letter we consider just a 2HDM, we nevertheless have a large number of parameters. In order to facilitate the numerical analysis it is useful to reduce that number. We adopt the strategy of [16] and assume the following:

A. There is no mixing between the two scalar doublets.

B. All parameters are real.

---

[2]The box diagrams for $\mu^- \to e^- e^+ e^-$ and $\tau^- \to \ell_2^- \ell_3^+ \ell_3^-$ are also suppressed by $1/m_R^2$ [15].

[3]It was already stressed in [27] (see also [28, 29]) that the radiative corrections to the seesaw mechanism, in the presence of two or more Higgs doublets and heavy neutral scalars, may be quite large. Moreover, it has been demonstrated in [30] that, even with only one Higgs doublet, those corrections may be substantial for fine-tuned tree-level neutrino mass matrices.

Through assumption A, the mixing of the scalars is simplified to [16]

$$\varphi_1^+ = G^+, \quad \varphi_2^+ = H^+, \quad \varphi_1^0 = \frac{v + H + iG^0}{\sqrt{2}}, \quad \varphi_2^0 = e^{-i\alpha} \frac{S_3^0 + iS_4^0}{\sqrt{2}}, \tag{1.4}$$

where H^+ is a physical charged scalar which, however, plays no role in this letter. The advantage of assumption A is threefold:

- There are in general three parameters in the mixing of the neutral scalars [16, 31]. With assumption A they are reduced to only one — the phase α, which is, however, unphysical because one may freely rephase φ_2^+ and φ_2^0.[4]

- The formulas for the BRs simplify considerably (see section 3).

- The couplings of H are identical to the ones in the SM, hence the experimental restrictions on the couplings of H are automatically fulfilled.

We thus consider that we are in the exact *alignment limit* of the 2HDM. This is in accordance with the measurements of the properties of the scalar discovered at LHC (see for instance [32, 33]), which have found that that scalar behaves in a manner very similar to the SM Higgs boson; its couplings are experimentally constrained to be very close to their respective SM values [34]. Assumption A ensures that this indeed happens in our 2HDM. In the ensuing discussions we will initially keep complex parameters, but we take into account assumption A right from the beginning.

This letter is organized as follows. In section 2 we discuss the light-neutrino mass matrix, including the radiative corrections. The formulas for the decay rates are displayed in section 3, where we also derive a prediction of our model when assumption A holds. In section 4 we discuss the procedure of our numerical investigation and in section 5 some results thereof are presented. We draw our conclusions in section 6. An appendix makes a digression through the scalar potential of the 2HDM in order to demonstrate that the two new scalars S_3^0 and S_4^0 may have sufficiently different masses.

2 The light-neutrino mass matrix

The Majorana mass matrix $\mathcal{M}_\nu$ of the light neutrinos is diagonalized as

$$U_L^T \mathcal{M}_\nu U_L = \hat{m} \equiv \mathrm{diag}\,(m_1, m_2, m_3), \tag{2.1}$$

where U_L is 3×3 unitary and the m_j $(j = 1, 2, 3)$ are real and non-negative. Since the charged-lepton mass matrix is diagonal from the start, cf. (1.2), U_L is just the lepton mixing matrix. The matrix M_R, defined in (1.3), is diagonalized as

$$U_R^\dagger M_R U_R^* = \widetilde{m} \equiv \mathrm{diag}\,(m_4, m_5, m_6), \tag{2.2}$$

---

[4]Due to assumption B, later on we will set $e^{-i\alpha} = 1$ in (1.4).

where the m_{3+j} are real and positive and the matrix U_R is 3×3 unitary. For the decay rates — see (3.1) in the next section — we need the quantities [15, 16]

$$X_{\ell_1 \ell_2} = \frac{1}{16\sqrt{2}\pi^2} \sum_{j=1}^{3} (U_R)_{\ell_1 j} (U_R^*)_{\ell_2 j} \ln \frac{m_{3+j}^2}{\mu^2} \tag{2.3}$$

for $\ell_1 \neq \ell_2$.[5] This requires us to know both U_R and the heavy-neutrino masses $m_{4,5,6}$. Note that, since U_R is a 3×3 unitary matrix, $X_{\ell_1 \ell_2}$ cannot be large; one has $|X_{\ell_1 \ell_2}| \lesssim 0.1$ if $10^9 \, \mathrm{GeV} \leq m_{4,5,6} \leq 10^{19} \, \mathrm{GeV}$.

We parameterize U_L as

$$U_L = e^{i\hat{\alpha}} \, U_{\mathrm{PMNS}} \, e^{i\hat{\beta}}, \tag{2.4a}$$

$$U_{\mathrm{PMNS}} = \begin{pmatrix} c_{12}c_{13} & s_{12}c_{13} & \epsilon^* \\ -s_{12}c_{23} - c_{12}s_{23}\,\epsilon & c_{12}c_{23} - s_{12}s_{23}\,\epsilon & s_{23}c_{13} \\ s_{12}s_{23} - c_{12}c_{23}\,\epsilon & -c_{12}s_{23} - s_{12}c_{23}\,\epsilon & c_{23}c_{13} \end{pmatrix}, \tag{2.4b}$$

$$\epsilon \equiv s_{13} \exp{(i\delta)}. \tag{2.4c}$$

In (2.4a), $e^{i\hat{\alpha}}$ and $e^{i\hat{\beta}}$ are diagonal matrices of phase factors while U_{PMNS} is the Pontecorvo-Maki-Nakagawa-Sakata matrix [4]. Out of the three phases in $e^{i\hat{\beta}}$, one may be absorbed into $\hat{\alpha}$ and the remaining two are the so-called Majorana phases, which are physically meaningful quantities. In (2.4b) and (2.4c), $c_{ij} = \cos{\theta_{ij}}$ and $s_{ij} = \sin{\theta_{ij}}$ for $ij = 12, 13, 23$, and δ is a CP-violating phase. The matrix U_R may be parameterized in the same way as U_L.

The matrix $\mathcal{M}_\nu$ is the sum of two parts:

$$\mathcal{M}_\nu = M_\nu^{\mathrm{tree}} + \delta M_L, \tag{2.5}$$

where the tree-level part M_ν^{tree} is given by the seesaw mechanism and the one-loop-level part δM_L is generated by the radiative corrections. As is well known,

$$M_\nu^{\mathrm{tree}} = -M_D^T M_R^{-1} M_D, \tag{2.6}$$

where M_D is the neutrino Dirac mass matrix. Referring to (1.2), let us define the diagonal matrices

$$\Delta_1 = \mathrm{diag}\,(d_e,\, d_\mu,\, d_\tau) \quad \mathrm{and} \quad \Delta_2 = \mathrm{diag}\,(\delta_e,\, \delta_\mu,\, \delta_\tau). \tag{2.7}$$

Because we use the Higgs basis, M_D is given by

$$M_D = \frac{v}{\sqrt{2}} \, \Delta_1, \tag{2.8}$$

hence it is diagonal. Thus,

$$M_\nu^{\mathrm{tree}} = -\frac{v^2}{2} \, \Delta_1 \, U_R^* \, \frac{1}{\widetilde{m}} \, U_R^\dagger \, \Delta_1. \tag{2.9}$$

---

[5]The renormalization scale μ that renders the argument of the logarithm dimensionless is arbitrary, since U_R is unitary and only the case $l_1 \neq l_2$ is considered in this work.

The radiative part of $\mathcal{M}_\nu$ is given by [26]

$$\delta M_L = \frac{3m_Z^2}{32\pi^2} \Delta_1 U_R^* \left(\frac{1}{\widetilde{m}} \ln \frac{\widetilde{m}^2}{m_Z^2} \right) U_R^\dagger \Delta_1 \tag{2.10a}$$

$$+ \frac{m_H^2}{32\pi^2} \Delta_1 U_R^* \left(\frac{1}{\widetilde{m}} \ln \frac{\widetilde{m}^2}{m_H^2} \right) U_R^\dagger \Delta_1 \tag{2.10b}$$

$$+ \frac{M_3^2}{32\pi^2} e^{-2i\alpha} \Delta_2 U_R^* \left(\frac{1}{\widetilde{m}} \ln \frac{\widetilde{m}^2}{M_3^2} \right) U_R^\dagger \Delta_2 \tag{2.10c}$$

$$- \frac{M_4^2}{32\pi^2} e^{-2i\alpha} \Delta_2 U_R^* \left(\frac{1}{\widetilde{m}} \ln \frac{\widetilde{m}^2}{M_4^2} \right) U_R^\dagger \Delta_2, \tag{2.10d}$$

where the four lines correspond successively to the contribution of the Z^0 gauge boson with mass m_Z, of the SM scalar H, and of the new scalars S_3^0 and S_4^0. In (2.10) we have already taken into account assumption A of section 1. We have also used $m_{4,5,6} \gg m_Z, m_H, M_{3,4}$. It is clear that for $M_{3,4} \gtrsim 4\pi v$ and provided Δ_1 and Δ_2 are of identical orders of magnitude, the contributions (2.10c) and (2.10d) dominate over the contribution (2.9) provided $M_3 \neq M_4$.[6] Lines (2.10c) and (2.10d) coincide with the well-known scotogenic mechanism; however, in the scotogenic model proper [35] the Yukawa couplings d_ℓ and γ_ℓ are zero (because of an additional symmetry), while in this letter they are nonzero.

We reformulate (2.1) to

$$e^{-i\hat{\alpha}} U_{\text{PMNS}}^* \left(\hat{m} \, e^{-2i\hat{\beta}} \right) U_{\text{PMNS}}^\dagger e^{-i\hat{\alpha}} = -\frac{v^2}{2} \Delta_1 U_R^* \frac{1}{\widetilde{m}} U_R^\dagger \Delta_1 \tag{2.11a}$$

$$+ \frac{3m_Z^2}{32\pi^2} \Delta_1 U_R^* \left(\frac{1}{\widetilde{m}} \ln \frac{\widetilde{m}^2}{m_Z^2} \right) U_R^\dagger \Delta_1 \tag{2.11b}$$

$$+ \frac{m_H^2}{32\pi^2} \Delta_1 U_R^* \left(\frac{1}{\widetilde{m}} \ln \frac{\widetilde{m}^2}{m_H^2} \right) U_R^\dagger \Delta_1 \tag{2.11c}$$

$$+ \frac{M_3^2}{32\pi^2} e^{-2i\alpha} \Delta_2 U_R^* \left(\frac{1}{\widetilde{m}} \ln \frac{\widetilde{m}^2}{M_3^2} \right) U_R^\dagger \Delta_2 \tag{2.11d}$$

$$- \frac{M_4^2}{32\pi^2} e^{-2i\alpha} \Delta_2 U_R^* \left(\frac{1}{\widetilde{m}} \ln \frac{\widetilde{m}^2}{M_4^2} \right) U_R^\dagger \Delta_2. \tag{2.11e}$$

Equation (2.11) is the basis for our numerical computations.

The diagonal matrix $e^{i\hat{\alpha}}$ in the left-hand side of (2.11) is irrelevant; indeed, it can be absorbed into U_R in the right-hand side, since Δ_1 and Δ_2 are diagonal matrices. In principle we use as input the Majorana phases, U_{PMNS}, $\hat{m}$, Δ_1, Δ_2, α, M_3, and M_4 (and additionally the fixed values $v = 246\,\text{GeV}$, $m_Z = 91\,\text{GeV}$, and $m_H = 125\,\text{GeV}$) and we solve (2.11) to find the three m_{3+j} and the nine parameters of the 3×3 unitary matrix U_R. All the matrices in (2.11) are 3×3 symmetric and complex; therefore, equation (2.11) is in effect a system of 12 real equations for the 12 unknowns — $m_{4,5,6}$ and the nine parameters of U_R — that we need for the computation of the $X_{\ell_1 \ell_2}$. We stress that this parameter counting only serves to demonstrate the theoretical possibility of obtaining the $X_{\ell_1 \ell_2}$ from equation (2.11); when one attempts to do it numerically, equation (2.11) may sometimes prove difficult or impossible to solve.

---

[6]The large logarithms of $m_{3+j}/M_{3,4}$ further enhance the contributions (2.10c) and (2.10d).

In practice, we reduce the number of parameters by applying assumption B, i.e. the *reality assumption*. Concretely, we set

$$e^{-i\hat{\alpha}} = e^{-2i\hat{\beta}} = \mathbb{1}, \tag{2.12a}$$

$$e^{i\delta} = -1 \text{ in } U_{\text{PMNS}}, \tag{2.12b}$$

$$e^{-2i\alpha} = 1, \tag{2.12c}$$

$$d_\ell \text{ real } (\ell = e, \mu, \tau), \tag{2.12d}$$

$$\delta_\ell \text{ real } (\ell = e, \mu, \tau). \tag{2.12e}$$

In (2.12b) we have opted for $\delta = \pi$, which is phenomenologically preferred over $\delta = 0$ [36–39]. Using the assumptions (2.12), the symmetric matrix in the left-hand side of (2.11) is real, hence it has just six degrees of freedom. Then, the matrix U_R may be written

$$U_R = U_R' \times \text{diag} \left(\epsilon_4, \, \epsilon_5, \, \epsilon_6 \right), \tag{2.13}$$

where $U_R' \in \text{SO}(3)$ is a real matrix parameterized by three angles and the ϵ_{3+j} may be either 1 or i. Equation (2.11) is then used to determine the three angles of U_R' and the three $\epsilon_{3+j}^2 \, m_{3+j}$; the latter are either positive, if $\epsilon_{3+j} = 1$, or negative, if $\epsilon_{3+j} = i$.

Let us take stock of the (real) parameters in the game, after having performed the simplification stated in the previous paragraph. From the neutrino oscillation data, both the two mass-squared differences among the three light-neutrino masses and the three mixing angles in U_{PMNS} are known and they are used as input. There are then 15 unknown parameters in (2.11): the lightest neutrino mass, *viz.* m_1 for normal ordering and m_3 for inverted ordering of the neutrino masses, $M_{3,4}$, d_ℓ, δ_ℓ, $\epsilon_{3+j}^2 \, m_{3+j}$ for $j = 1, 2, 3$, and the three angles in U_R. As we shall see in the next section, there are in addition the three parameters γ_ℓ, which do not appear in (2.11) but occur in the BRs.

3 Decay rates

Repeating the result of [16], the decay rates are given by

$$\Gamma \left(\mu^- \to e^- e^+ e^- \right) = \frac{m_\mu}{6144\pi^3} \left[\frac{3}{4} \left(\frac{1}{M_3^4} + \frac{1}{M_4^4} \right) + \frac{1}{2 M_3^2 M_4^2} \right]$$
$$\times |X_{\mu e}|^2 \, |\gamma_e|^2 \left(|A_{\mu e}|^2 + |A_{e\mu}|^2 \right), \tag{3.1a}$$

$$\Gamma \left(\tau^- \to e^- e^+ e^- \right) = \frac{m_\tau}{6144\pi^3} \left[\frac{3}{4} \left(\frac{1}{M_3^4} + \frac{1}{M_4^4} \right) + \frac{1}{2 M_3^2 M_4^2} \right]$$
$$\times |X_{\tau e}|^2 \, |\gamma_e|^2 \left(|A_{\tau e}|^2 + |A_{e\tau}|^2 \right), \tag{3.1b}$$

$$\Gamma \left(\tau^- \to e^- \mu^+ \mu^- \right) = \frac{m_\tau}{6144\pi^3} \left(\frac{1}{M_3^4} + \frac{1}{M_4^4} \right) |X_{\tau e}|^2 \, |\gamma_\mu|^2 \left(|A_{\tau e}|^2 + |A_{e\tau}|^2 \right), \tag{3.1c}$$

$$\Gamma \left(\tau^- \to \mu^- \mu^+ \mu^- \right) = \frac{m_\tau}{6144\pi^3} \left[\frac{3}{4} \left(\frac{1}{M_3^4} + \frac{1}{M_4^4} \right) + \frac{1}{2 M_3^2 M_4^2} \right]$$
$$\times |X_{\tau\mu}|^2 \, |\gamma_\mu|^2 \left(|A_{\tau\mu}|^2 + |A_{\mu\tau}|^2 \right), \tag{3.1d}$$

$$\Gamma \left(\tau^- \to \mu^- e^+ e^- \right) = \frac{m_\tau}{6144\pi^3} \left(\frac{1}{M_3^4} + \frac{1}{M_4^4} \right) |X_{\tau\mu}|^2 \, |\gamma_e|^2 \left(|A_{\tau\mu}|^2 + |A_{\mu\tau}|^2 \right), \tag{3.1e}$$

where we have used the approximation that the final-state charged leptons are massless, and

$$
\begin{aligned}
A_{\ell_1\ell_2} = {} & \frac{\sqrt{2}}{v} \left(m_{\ell_1}^2 - m_{\ell_2}^2 \right) m_{\ell_1} \delta_{\ell_1}^* d_{\ell_2} + m_{\ell_1}^2 \gamma_{\ell_1} \left(\delta_{\ell_1}^* \delta_{\ell_2} - d_{\ell_1}^* d_{\ell_2} \right) \\
& + \frac{m_{\ell_1} m_{\ell_2}}{2} \gamma_{\ell_2} \left(3 d_{\ell_1}^* d_{\ell_2} - \delta_{\ell_1}^* \delta_{\ell_2} \right) - \frac{m_{\ell_2}^2}{2} \gamma_{\ell_1} \left(\delta_{\ell_1}^* \delta_{\ell_2} + d_{\ell_1}^* d_{\ell_2} \right) \\
& + \frac{v}{\sqrt{2}} m_{\ell_2} \gamma_{\ell_1} \left(d_{\ell_1}^* \gamma_{\ell_2} \delta_{\ell_2} - \delta_{\ell_1}^* \gamma_{\ell_2}^* d_{\ell_2} \right) + \frac{v}{\sqrt{2}} m_{\ell_1} \left(\delta_{\ell_1}^* \left| \gamma_{\ell_2} \right|^2 d_{\ell_2} - \gamma_{\ell_1}^2 d_{\ell_1}^* \delta_{\ell_2} \right).
\end{aligned} \quad (3.2)
$$

We stress that assumption A is responsible for the relatively simple form of the decay rates.

3.1 A prediction

Taking ratios of decay rates of the τ, we obtain ratios of BRs. Defining

$$
x \equiv \left(\frac{M_3}{M_4} \right)^2 \quad \text{and} \quad y \equiv \left| \frac{\gamma_\mu}{\gamma_e} \right|^2, \quad (3.3)
$$

we obtain

$$
\frac{\text{BR}\left(\tau^- \to e^- \mu^+ \mu^- \right)}{\text{BR}\left(\tau^- \to e^- e^+ e^- \right)} = y \, \frac{4x^2 + 4}{3x^2 + 3 + 2x}, \quad (3.4\text{a})
$$

$$
\frac{\text{BR}\left(\tau^- \to \mu^- \mu^+ \mu^- \right)}{\text{BR}\left(\tau^- \to \mu^- e^+ e^- \right)} = y \, \frac{3x^2 + 3 + 2x}{4x^2 + 4}. \quad (3.4\text{b})
$$

This implies

$$
\sqrt{\frac{\text{BR}\left(\tau^- \to e^- e^+ e^- \right) \text{BR}\left(\tau^- \to \mu^- \mu^+ \mu^- \right)}{\text{BR}\left(\tau^- \to e^- \mu^+ \mu^- \right) \text{BR}\left(\tau^- \to \mu^- e^+ e^- \right)}} = \frac{3x^2 + 3 + 2x}{4x^2 + 4}. \quad (3.5)
$$

The maximum of the function in the right-hand side of (3.5) is 1 at $x = 1$; its minimum is $3/4$ at $x = 0$ and $x = \infty$. Therefore, we have the following *prediction*:

The ratio $\dfrac{\text{BR}\left(\tau^- \to e^- e^+ e^- \right) \text{BR}\left(\tau^- \to \mu^- \mu^+ \mu^- \right)}{\text{BR}\left(\tau^- \to e^- \mu^+ \mu^- \right) \text{BR}\left(\tau^- \to \mu^- e^+ e^- \right)}$ should lie between $\dfrac{9}{16}$ and 1.

This is a non-trivial result of our model, provided assumption A holds.

3.2 Suppressing $\mu^- \to e^- e^+ e^-$

With the mean lives τ_μ and τ_τ of muon and tau, respectively, it follows from (3.1) that

$$
R_{\text{BR}} \equiv \frac{\text{BR}\left(\mu^- \to e^- e^+ e^- \right)}{\text{BR}\left(\tau^- \to e^- e^+ e^- \right)} = \frac{\tau_\mu m_\mu}{\tau_\tau m_\tau} \, R_X R_A = 0.45 \times 10^6 \left(R_X R_A \right), \quad (3.6)
$$

where

$$
R_X \equiv \left| \frac{X_{\mu e}}{X_{\tau e}} \right|^2 \quad \text{and} \quad R_A \equiv \frac{\left| A_{\mu e} \right|^2 + \left| A_{e\mu} \right|^2}{\left| A_{\tau e} \right|^2 + \left| A_{e\tau} \right|^2}. \quad (3.7)
$$

The extant experimental upper bounds on the BRs are given in table 1. In the future, it is expected that the experimental sensitivity on BR $\left(\mu^- \to e^- e^+ e^- \right)$ will reach $\sim 10^{-16}$ [5], while the sensitivity on the BRs of the four LFV τ decays may be increased by one order of

BR $(\mu^- \rightarrow e^- e^+ e^-)$	<	1.0×10^{-12}
BR $(\tau^- \rightarrow e^- e^+ e^-)$	<	2.7×10^{-8}
BR $(\tau^- \rightarrow e^- \mu^+ \mu^-)$	<	2.7×10^{-8}
BR $(\tau^- \rightarrow \mu^- \mu^+ \mu^-)$	<	2.1×10^{-8}
BR $(\tau^- \rightarrow \mu^- e^+ e^-)$	<	1.8×10^{-8}

Table 1. The experimental upper bounds on the branching ratios. The bounds are 90% CL and have been taken from [4].

magnitude to $\sim 10^{-9}$ either at a Super B factory [6] or at the High Luminosity LHC [7, 8], and even reach $\sim 10^{-10}$ at Belle II [9].

We will be interested in obtaining parameter-space points for which all the BRs are below the extant experimental bounds but above the expected future sensitivities. Using the present experimental upper bound 10^{-12} on BR $(\mu^- \rightarrow e^- e^+ e^-)$ and taking, for definiteness, the future sensitivity on the BRs of the τ^- decays to be 10^{-9}, we obtain from (3.6) that

$$R_X R_A \lesssim 2 \times 10^{-9} \tag{3.8}$$

for such points. This may happen either because R_X is very small, or R_A is very small, or both. Focussing specifically on R_A, by using $m_{\ell_2} \ll m_{\ell_1} \ll v$ together with the assumption that all the Yukawa couplings are real, we read off from (3.2) the dominant terms

$$A_{\mu e} \approx \frac{v m_\mu}{\sqrt{2}} \left(\gamma_e^2 d_e \delta_\mu - \gamma_\mu^2 d_\mu \delta_e \right), \tag{3.9a}$$

$$A_{e\mu} \approx \frac{v m_\mu}{\sqrt{2}} \gamma_e \gamma_\mu \left(d_e \delta_\mu - d_\mu \delta_e \right). \tag{3.9b}$$

Therefore, in order to obtain a small R_A both $d_e \delta_\mu - d_\mu \delta_e$ and $\gamma_e^2 - \gamma_\mu^2$ should be small.

4 Numerical procedure

Solving (2.11) means finding m_4, m_5, m_6 and the matrix U_R. The latter is parameterized just as U_L in (2.4), i.e. its elements are given by

$$(U_R)_{11} = C_{12} C_{13} \exp\left[i \left(\alpha_1^R + \beta_1^R \right)\right], \tag{4.1a}$$

$$(U_R)_{12} = S_{12} C_{13} \exp\left[i \left(\alpha_1^R + \beta_2^R \right)\right], \tag{4.1b}$$

$$(U_R)_{13} = S_{13} \exp\left[i \left(\alpha_1^R + \beta_3^R - \delta^R \right)\right], \tag{4.1c}$$

$$(U_R)_{21} = \left[-S_{12} C_{23} - C_{12} S_{23} S_{13} \exp\left(i\delta^R \right) \right] \exp\left[i \left(\alpha_2^R + \beta_1^R \right)\right], \tag{4.1d}$$

$$(U_R)_{22} = \left[C_{12} C_{23} - S_{12} S_{23} S_{13} \exp\left(i\delta^R \right) \right] \exp\left[i \left(\alpha_2^R + \beta_2^R \right)\right], \tag{4.1e}$$

$$(U_R)_{23} = S_{23} C_{13} \exp\left[i \left(\alpha_2^R + \beta_3^R \right)\right], \tag{4.1f}$$

$$(U_R)_{31} = \left[S_{12} S_{23} - C_{12} C_{23} S_{13} \exp\left(i\delta^R \right) \right] \exp\left[i \left(\alpha_3^R + \beta_1^R \right)\right], \tag{4.1g}$$

$$(U_R)_{32} = \left[-C_{12} S_{23} - S_{12} C_{23} S_{13} \exp\left(i\delta^R \right) \right] \exp\left[i \left(\alpha_3^R + \beta_2^R \right)\right], \tag{4.1h}$$

$$(U_R)_{33} = C_{23} C_{13} \exp\left[i \left(\alpha_3^R + \beta_3^R \right)\right], \tag{4.1i}$$

where $S_{ij} = \sin\theta_{ij}^R$ and $C_{ij} = \cos\theta_{ij}^R$. However, following the reality assumption (2.12), the matrix in the left-hand side of (2.11) is real, hence U_R is real as well, apart from possible imaginary factors ϵ_{3+j} in (2.13). In order to avoid finding the same solutions of (2.11) several times in different conventions, we fix the phases in U_R as $\delta^R = \alpha_1^R = \alpha_2^R = \pi$ and $\alpha_3^R = \beta_1^R = \beta_2^R = \beta_3^R = 0$,[7] while simultaneously we allow the $\epsilon_{3+j}^2 m_{3+j}$ to be either positive or negative and the angles θ_{ij}^R to be in any quadrant.

The left-hand side of (2.11) is determined in the following way: choosing normal mass ordering of the light neutrinos,[8] the mass m_1 is an input and

$$m_2 = \sqrt{m_1^2 + \Delta m_{21}^2} \quad \text{and} \quad m_3 = \sqrt{m_1^2 + \Delta m_{31}^2}. \tag{4.2}$$

For the mass-squared differences and the mixing angles in U_{PMNS} we take the best-fit values of [36]:

$$
\begin{aligned}
\Delta m_{21}^2 &= 7.39 \times 10^{-5}\,\text{eV}^2, & \Delta m_{31}^2 &= 2.525 \times 10^{-3}\,\text{eV}^2, \\
\sin^2\theta_{12} &= 0.310, & \sin^2\theta_{13} &= 0.02241, & \sin^2\theta_{23} &= 0.580.
\end{aligned}
\tag{4.3}
$$

Our fitting program consists of two parts. In the first part, the matrix equation (2.11) is solved by using a minimization procedure wherein the function χ_{eq}^2, given in (4.4) below, is adjusted to zero with high precision. In this part of the program all the parameters that occur in the branching ratios, except the Yukawa couplings γ_ℓ, are determined. In the second part of the program, we use the parameters obtained in the first part and we search for γ_ℓ such that either several or all five branching ratios are within the future experimental reach; this is done with the help of the function χ_{br}^2 given in (4.6) below.

The function χ_{eq}^2 is constructed in the following way. Let $(\mathcal{M}_\nu^{\text{exp}})_{ij}$ and $\left(\mathcal{M}_\nu^{\text{theor}}\right)_{ij}$ be the matrix elements of the matrices in the left-hand and right-hand sides, respectively, of (2.11). Then, the function that we minimize is[9]

$$\chi_{\text{eq}}^2 = \sum_{1 \le i \le j \le 3} \left[\left(f_{ij}^{\text{mod}} \right)^2 + \left(f_{ij}^{\text{arg}} \right)^2 \right] \tag{4.4}$$

with

$$f_{ij}^{\text{mod}} = \frac{|(\mathcal{M}_\nu^{\text{exp}})_{ij}| - |\left(\mathcal{M}_\nu^{\text{theor}}\right)_{ij}|}{|(\mathcal{M}_\nu^{\text{exp}})_{ij}| + |\left(\mathcal{M}_\nu^{\text{theor}}\right)_{ij}|}, \tag{4.5a}$$

$$f_{ij}^{\text{arg}} = \begin{cases} \dfrac{\arg(\mathcal{M}_\nu^{\text{exp}})_{ij} - \arg\left(\mathcal{M}_\nu^{\text{theor}}\right)_{ij}}{\arg(\mathcal{M}_\nu^{\text{exp}})_{ij} + \arg\left(\mathcal{M}_\nu^{\text{theor}}\right)_{ij}} & \Leftarrow \arg(\mathcal{M}_\nu^{\text{exp}})_{ij} \ne 0, \\[2ex] \arg\left(\mathcal{M}_\nu^{\text{theor}}\right)_{ij} & \Leftarrow \arg(\mathcal{M}_\nu^{\text{exp}})_{ij} = 0. \end{cases} \tag{4.5b}$$

---

[7]This choice is arbitrary; in principle, many other phase fixings would be just as good.

[8]We have not considered the case of inverted mass ordering, which is disfavoured by the phenomenological fits. We note, however, that in a recent analysis [39] the preference for normal ordering has decreased.

[9]This function is appropriate for both cases of a complex or real $\mathcal{M}_\nu$; in our actual practice, we only use it in the real case.

In the first part of our fitting program we proceed in the following way. The mass-squared differences Δm_{21}^2 and Δm_{31}^2 and the lepton mixing angles θ_{12}, θ_{13}, and θ_{23} are fixed to their best-fit values [36]. In section 2 we have already stated the values of v, m_Z, and m_H used in our code. Nine parameters — the masses M_3 and M_4 of the new scalars, the mass m_1 of the lightest neutrino, and the real Yukawa couplings d_ℓ and δ_ℓ for $\ell = e, \mu, \tau$ — are inputted into (2.11); that matrix equation is solved by minimizing χ_{eq}^2 with respect to the six parameters θ_{ij}^R and $\epsilon_{3+j}^2 \, m_{3+j}$, which form the output of (2.11). We consider (2.11) to be solved when $\chi_{\text{eq}}^2 < 10^{-16}$; the resulting set of 15 parameters is then saved for usage in the second part of the fitting program.

Note that, since we use a minimization procedure, we may as well explore the full parameter space and minimize χ_{eq}^2 with respect to all 15 parameters simultaneously. It is also possible to choose any subspace in the 15-dimensional parameter space and to perform the minimization of χ_{eq}^2 in that subspace; indeed, in the following we shall do precisely this, by either fixing or imposing restrictions on the ranges of some of the input parameters prior to minimization of χ_{eq}^2.

The function χ_{br}^2 is constructed in the following way:

$$
\chi_{\text{br}}^2 = \sum_{i=1}^{5} \left[\Theta \left(\text{BR}_i^{\text{bound}} - \text{BR}_i^{\text{theor}} \right) \left(\frac{\text{BR}_i^{\text{bound}}}{\text{BR}_i^{\text{theor}}} \right)^2 \right.
$$
$$
\left. + \Theta \left(\text{BR}_i^{\text{theor}} - \text{BR}_i^{\text{bound}} \right) \left(\frac{\text{BR}_i^{\text{theor}} - \text{BR}_i^{\text{bound}}}{k} \right)^2 \right], \tag{4.6}
$$

where the index i runs over the five BRs, Θ is the Heaviside step function, $\text{BR}_i^{\text{bound}}$ denotes the experimental upper bound on each BR (these are the bounds given in table 1), $\text{BR}_i^{\text{theor}}$ is the calculated value of the BR, and k is a small number that is meant to give a kick to the minimization algorithm whenever the calculated value is larger than the experimental upper bound. Note that the minimum possible value of χ_{br}^2 is five, which materializes in the limit where all five calculated BRs are just a little smaller than the experimental bound on the corresponding BR.[10] The minimization function (4.6) can handle even situations when the calculated BRs and the upper experimental bounds differ by many orders of magnitude. The function χ_{br}^2 is minimized only with respect to the Yukawa couplings γ_ℓ, because the other parameters have been fixed already in the first part of the fitting program. We stress that, in contrast to χ_{eq}^2, it is not necessary to minimize χ_{br}^2 with high precision, since our objective is to obtain BRs that are *below* but not necessarily close to their respective experimental bounds. We use 10^{-16} and 10^{-9} as the future experimental sensitivities on $\text{BR}\left(\mu^- \to e^- e^+ e^-\right)$ and the BRs of the τ^- decays, respectively.

---

[10]One might object that by minimizing the function (4.6) one would almost always end up with points having all the computed $\text{BR}_i^{\text{theor}}$ very close to their respective present experimental upper bounds $\text{BR}_i^{\text{bound}}$. This does not happen, though, because it is quite difficult to reach the minimum value 5 of χ_{br}^2 by just varying the three parameters $\gamma_{e,\mu,\tau}$. Actually, as one can check for instance by looking at figure 4 below, even after minimizing χ_{br}^2 we obtain lots of points with $\text{BR}_i^{\text{theor}} \ll \text{BR}_i^{\text{bound}}$ for some of the five decays.

Often, we want to compare the results of equation (2.11) with the ones of its tree-level counterpart

$$e^{-i\hat{\alpha}} U_{\text{PMNS}}^* \left(\hat{m}\, e^{-2i\hat{\beta}} \right) U_{\text{PMNS}}^\dagger\, e^{-i\hat{\alpha}} = -\frac{v^2}{2}\, \Delta_1\, U_R^*\, \frac{1}{\widetilde{m}}\, U_R^\dagger\, \Delta_1. \tag{4.7}$$

Whenever we perform such a comparison, we use the superscript "(loop)" on quantities that arise from the solution of (2.11) and the superscript "(tree)" on quantities that arise from the solution of (4.7). It is one objective of this letter to show that the quantities with superscript "(loop)" may be substantially different from the corresponding quantities with superscript "(tree)".

5 Results

5.1 Evolution of the $X_{\ell_1 \ell_2}$

In this subsection we give two examples of the way the quantities $X_{\ell_1 \ell_2}$ may change when the input parameters are varied.

In our first example we fix eight inputs as follows: $m_1 = 30\,\text{meV}$, $M_3 = 1.5\,\text{TeV}$, $M_4 = 1.6\,\text{TeV}$,[11] $d_e = 0.01$, $d_\mu = 0.1$, $d_\tau = 0.001$, $\delta_e = 1$, and $\delta_\mu = 0.001$. We vary δ_τ from 0.005 to 0.5 and compute $X_{\mu e}$, $X_{\tau e}$, and $X_{\tau \mu}$ for each value of δ_τ. In this case Δ_1 is kept fixed, hence the solution of (4.7) is always the same and produces $X_{\mu e}^{(\text{tree})} = 0.000232$, $X_{\tau e}^{(\text{tree})} = 0.000328$, $X_{\tau \mu}^{(\text{tree})} = -0.000260$, and heavy-neutrino masses $m_4^{(\text{tree})} = 7.18 \times 10^8\,\text{GeV}$, $m_5^{(\text{tree})} = 9.83 \times 10^{10}\,\text{GeV}$, and $m_6^{(\text{tree})} = 7.16 \times 10^{12}\,\text{GeV}$. In figure 1 we display the corresponding quantities with "(loop)" superscript. In particular, one observes in the top-left panel of that figure that $X_{\mu e}^{(\text{loop})}$ is zero for $\delta_\tau \simeq 0.1$. In the top-right panel of figure 1 one sees that both $X_{\mu e}^{(\text{loop})}$ and $X_{\tau \mu}^{(\text{loop})}$ are one order of magnitude larger than the corresponding tree-level quantities when $\delta_\tau \lesssim 0.01$, and the same happens for $X_{\tau e}$ when $\delta_\tau \gtrsim 0.2$. In the bottom panel of figure 1 one sees that all three heavy neutrinos are heavier when their masses are computed by taking into account the loop corrections; for instance, $m_6^{(\text{loop})} \sim 10^{15}\,\text{GeV}$ while $m_6^{(\text{tree})} < 10^{13}\,\text{GeV}$.

In our second example we fix eight input parameters as follows: $m_1 = 30\,\text{meV}$, $M_3 = 1.5\,\text{TeV}$, $M_4 = 1.6\,\text{TeV}$, $d_e = 0.01$, $d_\mu = 0.1$, $\delta_e = 1$, $\delta_\mu = 0.001$, and $\delta_\tau = 0.1$. We vary d_τ from 0.005 to 0.5 and we solve both (2.11) and (4.7) for each value of d_τ. The results obtained for the heavy-neutrino masses m_{3+j} are depicted in figure 2, at the loop level in the left panel and at tree level in the right one. One sees that, in the tree-level solution, the heavy-neutrino masses have a very simple behaviour: for low d_τ, $m_4^{(\text{tree})}$ increases with d_τ while $m_5^{(\text{tree})}$ and $m_6^{(\text{tree})}$ remain almost constant (in reality, they also increase but very slowly); then, for intermediate d_τ, it is $m_5^{(\text{tree})}$ that increases at a regular pace while $m_4^{(\text{tree})}$ and $m_6^{(\text{tree})}$ remain constant; finally, for high d_τ, $m_6^{(\text{tree})}$ increases but $m_4^{(\text{tree})}$ and $m_5^{(\text{tree})}$ are stable. Including the radiative corrections (left panel of figure 2) the whole picture changes; all three heavy-neutrino masses become one or two orders of magnitude larger, and moreover $m_5^{(\text{loop})}$ and $m_6^{(\text{loop})}$ exhibit a peculiar behaviour, interchanging positions at

---

[11]M_3 and M_4 must be rather close to each other, because their difference comes from a coupling in the scalar potential that is bounded by unitarity. See appendix A for details.
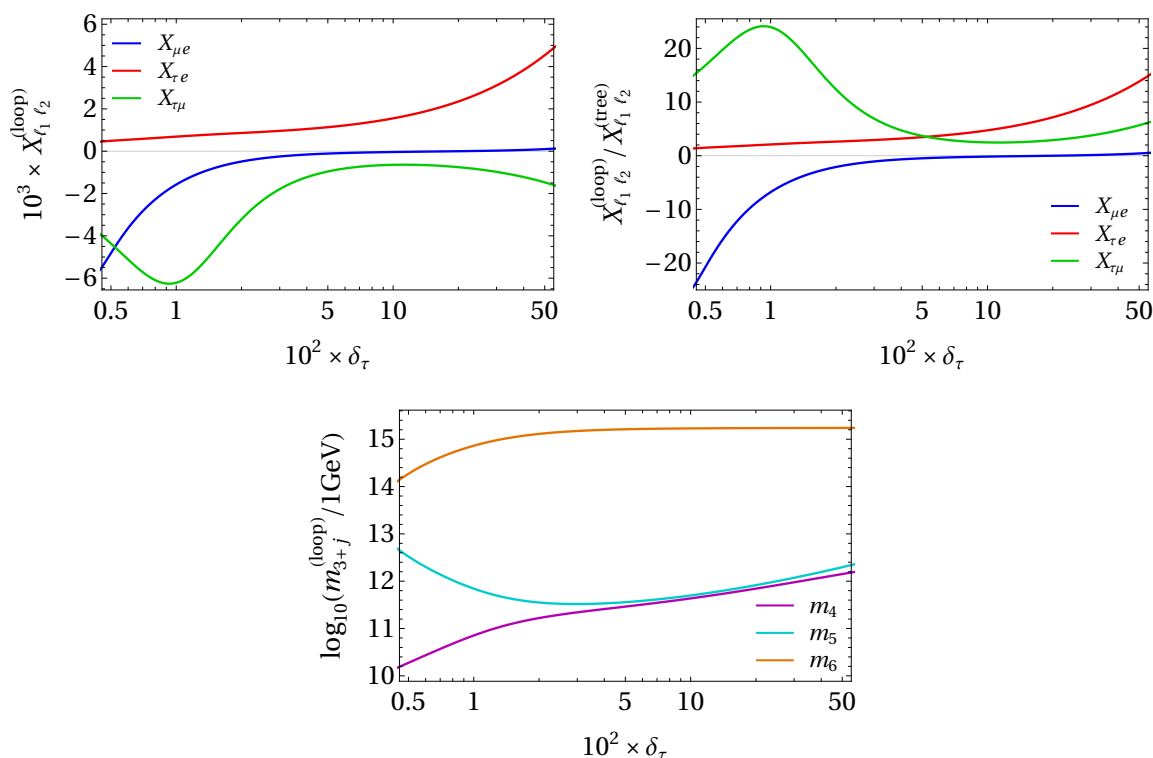
Figure 1. $X_{\ell_1 \ell_2}^{(\mathrm{loop})}$ (top-left panel), $X_{\ell_1 \ell_2}^{(\mathrm{loop})} / X_{\ell_1 \ell_2}^{(\mathrm{tree})}$ (top-right panel), and $m_{4,5,6}^{(\mathrm{loop})}$ (bottom panel) against δ_τ in a case where all other input parameters are kept fixed at values given in the main text. The definition of the quantities $X_{\ell_1 \ell_2}$ is given in (2.3); the definition of the right-handed neutrino masses $m_{4,5,6}$ is in (2.2); the Yukawa coupling δ_τ is defined in (2.7).
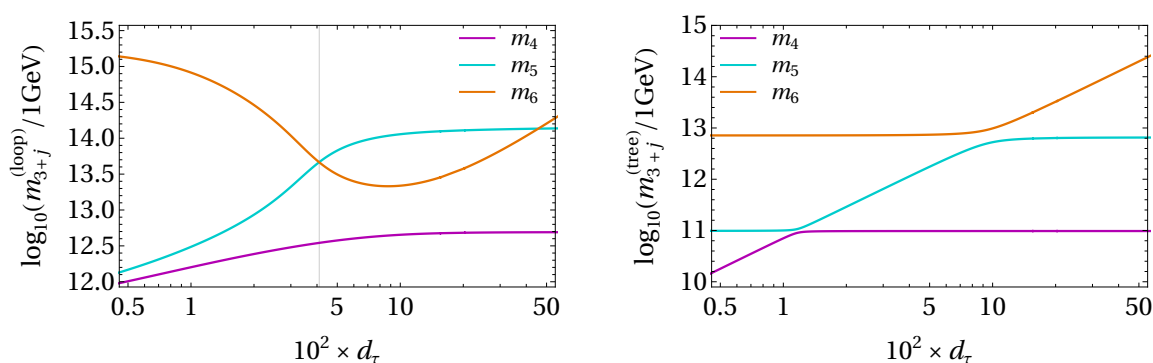
Figure 2. $m_{4,5,6}^{(\mathrm{loop})}$ (left panel) and $m_{4,5,6}^{(\mathrm{tree})}$ (right panel) against d_τ in a case where all other input parameters are kept fixed at values given in the main text. The Yukawa coupling d_τ is defined in (2.7).
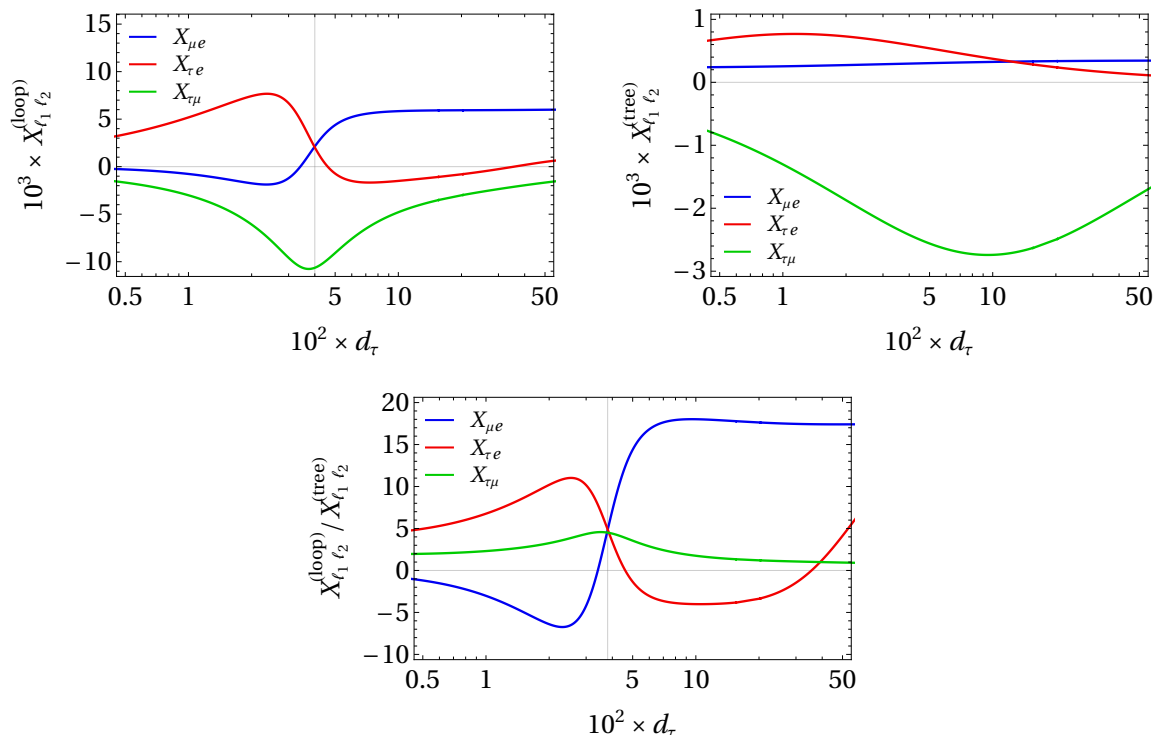
Figure 3. $X_{\ell_1\ell_2}^{(\text{loop})}$ (top-left panel), $X_{\ell_1\ell_2}^{(\text{tree})}$ (top-right panel), and $X_{\ell_1\ell_2}^{(\text{loop})}/X_{\ell_1\ell_2}^{(\text{tree})}$ (bottom panel) against d_τ, with the same input as in figure 2.

$d_\tau \approx 0.04$ and then again at $d_\tau \approx 0.45$. This peculiar behaviour of $m_{5,6}^{(\text{loop})}$ has a counterpart in the behaviour of the $X_{\ell_1\ell_2}^{(\text{loop})}$ depicted in the top-left panel of figure 3. One sees that both $X_{\mu e}^{(\text{loop})}$ and $X_{\tau e}^{(\text{loop})}$ experience sudden changes close to the point where $m_5^{(\text{loop})}$ and $m_6^{(\text{loop})}$ first interchange positions. One moreover sees that $X_{\tau e}^{(\text{loop})}$ is zero for two different values of d_τ, while $X_{\mu e}^{(\text{loop})}$ is zero only once. In the bottom panel of figure 3 one sees that the $X_{\ell_1\ell_2}^{(\text{loop})}/X_{\ell_1\ell_2}^{(\text{tree})}$ are typically of order 10, but both $X_{\tau e}^{(\text{loop})}/X_{\tau e}^{(\text{tree})}$ and $X_{\mu e}^{(\text{loop})}/X_{\mu e}^{(\text{tree})}$ have zeros. It is amusing to note that all three $X_{\ell_1\ell_2}^{(\text{loop})}/X_{\ell_1\ell_2}^{(\text{tree})}$ have approximately the same value at the first point where $m_5^{(\text{loop})}$ and $m_6^{(\text{loop})}$ cross.

5.2 Scatter plots of BRs

In figure 4 we present scatter plots of the branching ratios of[12] $\mu^- \to e^- e^+ e^-$, $\tau^- \to e^- e^+ e^-$, and $\tau^- \to \mu^- \mu^+ \mu^-$ as functions of m_1. Here as elsewhere in this section we always assume, for the sake of simplicity, the neutrino mass ordering to be normal. To produce the scatter plots, we chose m_1 at random in between 10^{-2} meV to 30 meV, prior to the minimization of χ_{eq}^2; larger values of m_1 would violate the *Planck* 2018 cosmological bound on the sum of the light-neutrino masses [40]. Then the BRs are computed, as described in section 4, by consecutive minimization of χ_{eq}^2 and χ_{br}^2 with respect to the remaining parameters. We

---

[12]As seen in (3.4), in our model the branching ratio of $\tau^- \to e^- \mu^+ \mu^-$ is closely related to the one of $\tau^- \to e^- e^+ e^-$, and the branching ratio of $\tau^- \to \mu^- e^+ e^-$ is related to the one of $\tau^- \to \mu^- \mu^+ \mu^-$. For this reason and in order to save space, we omit figures for BR $\left(\tau^- \to e^- \mu^+ \mu^-\right)$ and for BR $\left(\tau^- \to \mu^- e^+ e^-\right)$.
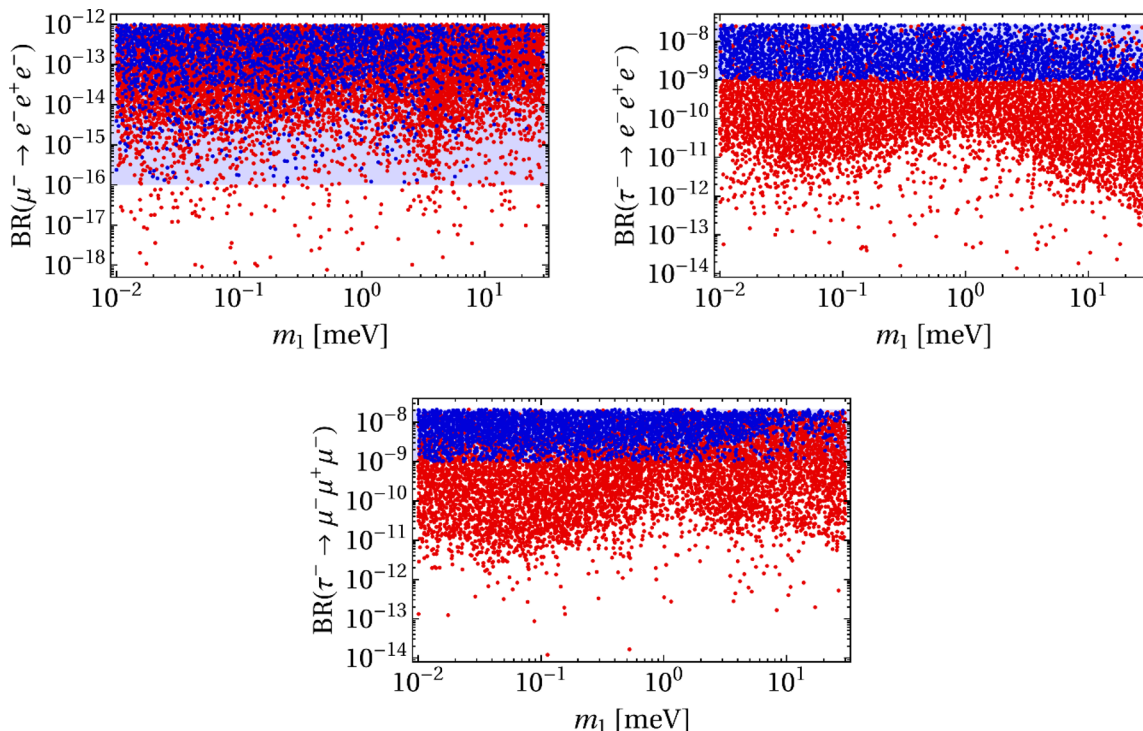
Figure 4. Scatter plots of $\mathrm{BR}\left(\mu^- \to e^- e^+ e^-\right)$ (top-left panel), $\mathrm{BR}\left(\tau^- \to e^- e^+ e^-\right)$ (top-right panel), and $\mathrm{BR}\left(\tau^- \to \mu^- \mu^+ \mu^-\right)$ (bottom panel) as functions of the lightest-neutrino mass m_1; the other inputs are given in (5.1) and (5.2). In all the displayed points, all five BRs satisfy the present experimental bounds given in table 1. Blue points have all five BRs larger than the expected future sensitivities, while red points allow one or more (but not all) BRs to be below the future sensitivities. The shadowed bands show the ranges between the present experimental bounds and the future experimental sensitivities, *viz.* 10^{-16} for $\mathrm{BR}\left(\mu^- \to e^- e^+ e^-\right)$ and 10^{-9} for the BRs of the τ^- decays.

restrict the parameter space by adopting the boundary conditions

$$750\,\mathrm{GeV} < M_{3,4} < 2\,\mathrm{TeV}, \tag{5.1a}$$

$$M_3^2 - \frac{8\pi}{3}\,v^2 < M_4^2 < M_3^2 + \frac{8\pi}{3}\,v^2, \tag{5.1b}$$

$$0.05 \le |d_\ell|\,,\,|\delta_\ell|\,,\,|\gamma_\ell| \le 0.5 \quad (\ell = e, \mu, \tau), \tag{5.1c}$$

and

$$10^{11}\,\mathrm{GeV} \le m_{4,5,6} \le 10^{16}\,\mathrm{GeV}, \tag{5.2}$$

with the $\epsilon_{3+j}^2\,m_{3+j}$ being either positive or negative. Notice that the range of Yukawa couplings that we have considered in (5.1c) is quite restricted compared to the Yukawa couplings of the charged fermions, that are known to vary from $\sim 10^{-6}$ to ~ 1.

It is worth making a number of comments concerning (5.1) and (5.2):

1. The lower bound on M_3 and M_4 that we have assumed in (5.1a) agrees roughly with the results of a recent analysis [41] of 2HDMs furnished with an additional $\mathbb{Z}_2$ symmetry.
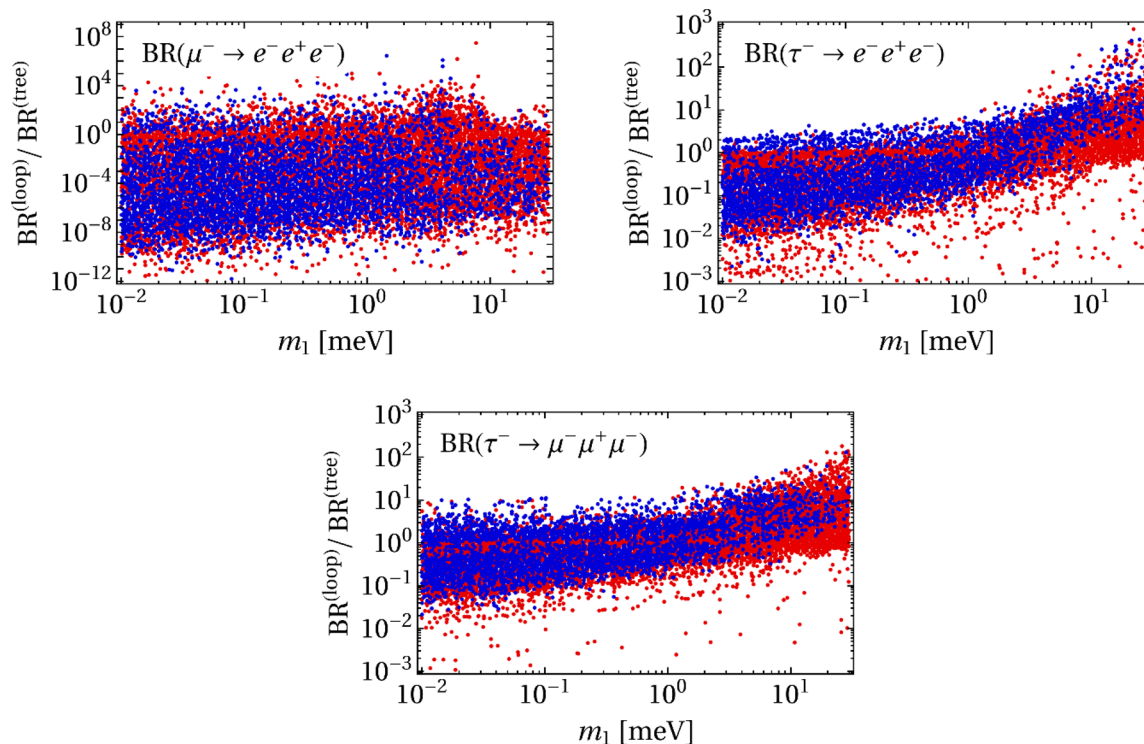
Figure 5. Scatter plots of $\mathrm{BR}^{(\mathrm{loop})}/\mathrm{BR}^{(\mathrm{tree})}$ for the decays $\mu^- \to e^- e^+ e^-$ (top-left panel), $\tau^- \to e^- e^+ e^-$ (top-right panel), and $\tau^- \to \mu^- \mu^+ \mu^-$ (bottom panel). The points are the ones used in figure 4, with the same colour coding as there.

2. In (5.1b) the bounds on M_4 have been chosen in such a way that all the relevant conditions on the 2HDM scalar potential are met. Namely, the difference between M_3^2 and M_4^2 originates in a coupling of the scalar potential that is bounded by unitarity, and therefore $|M_3^2 - M_4^2|$ cannot be too large. See appendix A for details.

3. Sometimes the solution of (2.11) requires one of the m_{3+j} to be very large, even divergent. This is not surprising because, when e.g. $m_6 \to \infty$, the contribution of m_6 to (2.11) simply vanishes. Unfortunately, though, when $m_6 \to \infty$ the $X_{\ell_1 \ell_2}$ diverge. We avoid this problem by discarding, through the upper bound in (5.2), those points where the solution of (2.11) requires very large m_{3+j}.

4. We have obtained points with values of the heavy-neutrino masses as low as 10^9 GeV. However, those points have very low BRs for the decays of the τ^-, of order 10^{-12}. In (5.2) we have discarded those points by enforcing a lower bound on the heavy-neutrino masses.

In figure 5 we display the ratios $\mathrm{BR}^{(\mathrm{loop})}\big/\mathrm{BR}^{(\mathrm{tree})}$ for the same points as in figure 4 and with the same colour notation. One sees that for the τ^- decays the BRs derived from (2.11) may easily be one or two orders of magnitude either above or below the corresponding BRs derived from (4.7). For the decay $\mu^- \to e^- e^+ e^-$ things may be much more dramatic, with differences of several orders of magnitude; this happens because either $X_{\mu e}^{(\mathrm{loop})}$ or
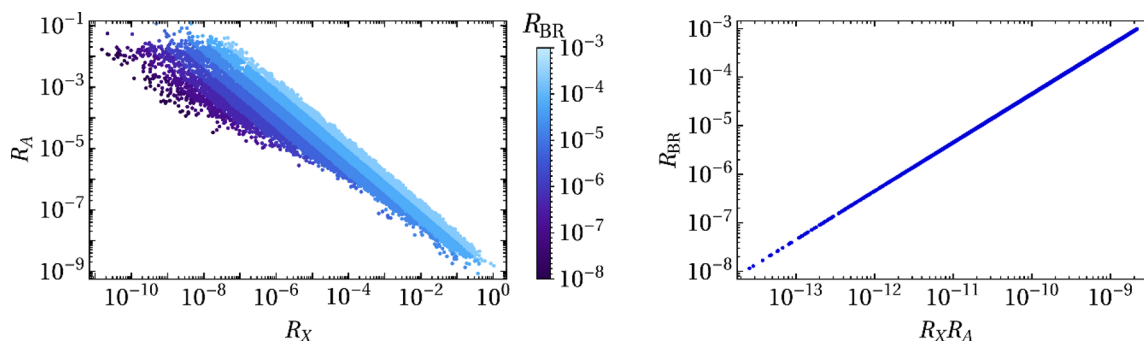
Figure 6. Scatter plots of R_A *vs.* R_X (left panel) and of their product $R_X R_A$ *vs.* R_{BR} (right panel) for the blue points of figure 4. The definitions of R_A, R_X, and R_{BR} are given in (3.6) and (3.7).

$X_{\mu e}^{(\mathrm{tree})}$ frequently become zero. It is worth mentioning that by allowing for wider ranges of the Yukawa couplings (for example, allowing $|d_\ell|$, $|\delta_\ell|$, and $|\gamma_\ell|$ to be between 0.001 and 1) would lead to the ratios $\mathrm{BR}^{(\mathrm{loop})} \big/ \mathrm{BR}^{(\mathrm{tree})}$ being sometimes much larger; those ratios could be two orders of magnitude larger or smaller than is shown in figure 5.

5.3 The suppression of $\mu^- \to e^- e^+ e^-$

In figure 6 we reuse the blue points of the previous figures 4 and 5, *viz.* points for which all five BRs are in between the respective present upper bounds and future expected sensitivities. For those points, we display R_{BR} defined in (3.6), and R_X and R_A defined in (3.7). In the right panel one sees that the inequality (3.8) holds and that $R_X R_A$ is proportional to R_{BR} as stated in (3.6). In the left panel one sees that the smallness of $R_X R_A$ most of the time occurs because both R_A and R_X are small, but there is a non-negligible fraction of points where one of them is extremely small and the other one is not small.

The discussion at the end of section 3.2 suggests that the smallness of R_A is correlated with the smallness of the asymmetries

$$A_1 \equiv \frac{d_e \delta_\mu - d_\mu \delta_e}{d_e \delta_\mu + d_\mu \delta_e} \quad \text{and} \quad A_2 \equiv \frac{\gamma_e^2 - \gamma_\mu^2}{\gamma_e^2 + \gamma_\mu^2}. \tag{5.3}$$

Using the same points as in figure 6, these asymmetries are displayed in figure 7. One sees that A_1 and A_2 are indeed very small when $R_A \lesssim 10^{-7}$, but they may be largish for R_A above that value; we remind the reader that, like we saw in figure 6, the smallness of $R_X R_A$ is often due to the smallness of R_X and not to the smallness of R_A, or vice-versa.

5.4 Benchmark points

In table 2 we produce three benchmark points. The first nine lines of that table contain the input to (2.11), *viz.* the matrices Δ_1 and Δ_2, the lightest-neutrino mass m_1, and the new-scalar masses M_3 and M_4. In the next six lines of table 2 one sees the output of (2.11), *viz.* the heavy-neutrino masses $\epsilon_{3+j}^2 m_{3+j}$ and the angles θ_{ij}^R that parameterize the matrix U_R. In the next three lines of table 2 one finds the parameters γ_ℓ that we have fitted in order to obtain the desirable branching ratios which are in the ensuing five lines of the table.
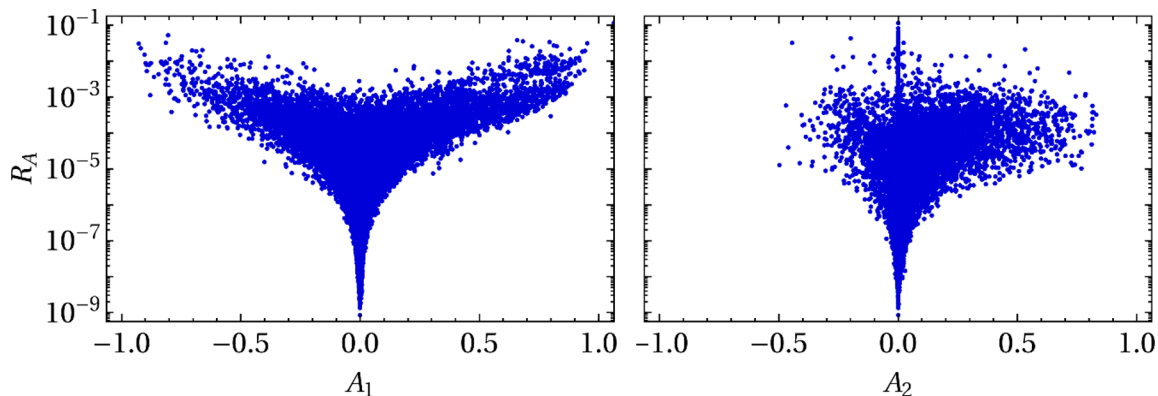
Figure 7. Scatter plots of A_1 (left panel) and A_2 (right panel) against R_A for the blue points of figure 4. The definitions of A_1 and A_2 are given in (5.3).

Finally, in the last three lines of table 2 we compare the values of the quantities $X_{\ell_1\ell_2}^{(\text{loop})}$ that were obtained from the solution of the one-loop equation (2.11) to the quantities $X_{\ell_1\ell_2}^{(\text{tree})}$ that result from the solution to the tree-level equation (4.7).

All the points in table 2 have small A_2 asymmetries. The asymmetry A_1 is also small for point 1, but not for points 2 and 3; the latter points rely on very small $X_{\mu e}^{(\text{loop})}$ to suppress $\mathrm{BR}(\mu^- \to e^- e^+ e^-)$.

6 Conclusions

The predictions for the lepton-flavour-violating charged-lepton decays may be used to discriminate among theoretical models. For instance, it has been found [43] that, in a model with a heavy charged gauge boson, the present bounds on $\mu^- \to e^- \gamma$ and $\mu^- \to e^- e^+ e^-$ restrict the parameters of the model in such a way that the decays $\tau^- \to \ell_2^- \ell_3^+ \ell_3^-$ ($\ell_2, \ell_3 = e, \mu$) will be invisible in the foreseeable future. In this letter we have considered a model with radically different predictions. In our model, LFV decays like $\mu^- \to e^- \gamma$ and $Z \to e^+ \mu^-$ are invisible, while $\mu^- \to e^- e^+ e^-$ and $\tau^- \to \ell_2^- \ell_3^+ \ell_3^-$ might be observed in future experiments.

Here we have investigated the one-loop radiative corrections to the light-neutrino mass matrix and their impact on the branching ratios $\mathrm{BR}\left(\ell_1^- \to \ell_2^- \ell_3^+ \ell_3^-\right)$. That impact occurs because the radiative corrections strongly influence the evaluation of the heavy-neutrino masses $m_{4,5,6}$ and of the mixing matrix U_R of the heavy neutrinos. In our model $\mathrm{BR}\left(\ell_1^- \to \ell_2^- \ell_3^+ \ell_3^-\right)$ is proportional to $|X_{\ell_1\ell_2}|^2$, where the quantities $X_{\ell_1\ell_2}$ defined in (2.3) depend on $m_{4,5,6}$ and U_R.

We have shown that the one-loop radiative corrections to the light-neutrino mass matrix may modify that matrix so much that the model's predictions for $\mu^- \to e^- e^+ e^-$ and $\tau^- \to \ell_2^- \ell_3^+ \ell_3^-$ change drastically. This is especially true for $\mathrm{BR}\left(\mu^- \to e^- e^+ e^-\right)$, which may shift by several orders of magnitude when one (dis)considers the effect of the radiative corrections on the determination of the heavy-neutrino masses and mixings. This happens, in particular, because $X_{\mu e}$ may be zero for different values of the model's parameters at the tree level and at the one-loop level. The predictions for the four decays $\tau^- \to \ell_2^- \ell_3^+ \ell_3^-$

	Point 1	Point 2	Point 3
d_e	-0.1007921873	-0.4760159332	-0.1486369437
d_μ	-0.1008806975	-0.3515469881	-0.1350920928
d_τ	0.4284126498	-0.1867255478	0.4815723378
δ_e	0.2866985699	0.06004123429	-0.4967063119
δ_μ	0.2867857061	-0.4838389436	0.1463403266
δ_τ	-0.05682546538	-0.4996927131	-0.4386169548
m_1 (meV)	19.97920246	21.24771538	0.01193047926
M_3 (GeV)	$1\,850.763353$	$1\,687.165806$	948.4168772
M_4 (GeV)	$1\,907.962751$	$1\,753.477583$	822.8728412
$\epsilon_4^2 m_4$ (GeV)	$-1.431876108 \times 10^{14}$	$-7.187027731 \times 10^{15}$	$8.630665168 \times 10^{13}$
$\epsilon_5^2 m_5$ (GeV)	$-4.522247054 \times 10^{13}$	$-1.190583685 \times 10^{14}$	$6.484748230 \times 10^{12}$
$\epsilon_6^2 m_6$ (GeV)	$9.182836790 \times 10^{15}$	$-3.431144882 \times 10^{14}$	$2.627559538 \times 10^{15}$
θ_{12}^R (rad)	2.974230185	3.940376049	0.2251793380
θ_{13}^R (rad)	3.322622001	2.779495689	1.533482136
θ_{23}^R (rad)	2.520334568	1.410325430	6.126970300
γ_e	0.499	0.5	0.4
γ_μ	0.5	-0.5	-0.34
γ_τ	-0.5	0.05	0.49
$\mathrm{BR}(\mu^- \to e^- e^+ e^-)$	4.9×10^{-13}	4.0×10^{-13}	3.0×10^{-13}
$\mathrm{BR}(\tau^- \to e^- e^+ e^-)$	1.1×10^{-9}	2.4×10^{-8}	2.5×10^{-9}
$\mathrm{BR}(\tau^- \to e^- \mu^+ \mu^-)$	1.1×10^{-9}	2.4×10^{-8}	1.9×10^{-9}
$\mathrm{BR}(\tau^- \to \mu^- \mu^+ \mu^-)$	1.5×10^{-8}	1.0×10^{-9}	1.1×10^{-9}
$\mathrm{BR}(\tau^- \to \mu^- e^+ e^-)$	1.5×10^{-8}	1.0×10^{-9}	1.5×10^{-9}
$X_{\mu e}^{(\text{loop})}/X_{\mu e}^{(\text{tree})}$	-2.69	$-1/505$	$1/1020$
$X_{\tau e}^{(\text{loop})}/X_{\tau e}^{(\text{tree})}$	8.02	20.3	$1/21.2$
$X_{\tau \mu}^{(\text{loop})}/X_{\tau \mu}^{(\text{tree})}$	7.93	1.33	$1/1.39$

Table 2. Three benchmark points.

usually change by no more than two orders of magnitude when one takes into account the radiative corrections, but for values of the Yukawa couplings larger than the ones displayed in figure 4 and given in (5.1c), the effects on $\mathrm{BR}\left(\tau^- \to \ell_2^- \ell_3^+ \ell_3^-\right)$ may be dramatic too.

Our work highlights the necessity of taking into account the one-loop radiative corrections to the light-neutrino mass matrix when making any numerical assessment or prediction of an effect that involves the masses $m_{4,5,6}$ and the mixing matrix U_R. Usage of the standard seesaw formula (2.6) is not adequate when one looks for detailed numerical predictions because the 'scotogenic-type' contributions to δM_L in (2.10c) and (2.10d) may

be non-negligible or even dominant. This happens even when one takes into account the restrictions posed by unitarity of the scalar potential on the squared-mass differences among the neutral scalars; though those differences are rather small, the effects of the radiative corrections are nevertheless large in general.

Acknowledgments

A The maximum possible value of $\left| M_3^2 - M_4^2 \right|$

In this appendix we study in detail the scalar potential of the 2HDM with alignment. Our purpose is to demonstrate that the difference between the squared masses of the two new neutral scalars of that model may reach $v^2 \left(8\pi/3 \right) \approx 5.07 \times 10^5 \, \text{GeV}^2$. We do not claim this to be an absolute upper bound; simply, we were able to demonstrate analytically that it may be reached. On the other hand, numerical scans that two of us have performed [42] suggest that $8\pi/3$ is indeed the maximum possible value of the parameter λ_5 of the scalar potential, even in the general case without alignment.

A.1 The scalar potential of the 2HDM

Let the two doublets be $\Phi_1 = \left(\varphi_1^+, \, \varphi_1^0 \right)^T$ and $\Phi_2 = \left(\varphi_2^+, \, \varphi_2^0 \right)^T$. The scalar potential is [17]

$$V = \mu_1 \, \Phi_1^\dagger \Phi_1 + \mu_2 \, \Phi_2^\dagger \Phi_2 + \left(\mu_3 \, \Phi_1^\dagger \Phi_2 + \text{H.c.} \right) \tag{A.1a}$$

$$+ \frac{\lambda_1}{2} \left(\Phi_1^\dagger \Phi_1 \right)^2 + \frac{\lambda_2}{2} \left(\Phi_2^\dagger \Phi_2 \right)^2 + \lambda_3 \, \Phi_1^\dagger \Phi_1 \, \Phi_2^\dagger \Phi_2 + \lambda_4 \, \Phi_1^\dagger \Phi_2 \, \Phi_2^\dagger \Phi_1 \tag{A.1b}$$

$$+ \left[\frac{\lambda_5}{2} \left(\Phi_1^\dagger \Phi_2 \right)^2 + \left(\lambda_6 \, \Phi_1^\dagger \Phi_1 + \lambda_7 \, \Phi_2^\dagger \Phi_2 \right) \Phi_1^\dagger \Phi_2 + \text{H.c.} \right], \tag{A.1c}$$

where $\mu_{1,2}$ and $\lambda_{1,\ldots,4}$ are real while μ_3 and $\lambda_{5,\ldots,7}$ are in general complex. It is convenient to define

$$\lambda_\pm := \frac{\lambda_1 \pm \lambda_2}{2} \quad \text{and} \quad \bar{\lambda}_\pm := \lambda_6 \pm \lambda_7. \tag{A.2}$$

The coefficients $\lambda_{1,\ldots,7}$ are subject to two types of conditions: the unitarity conditions and the boundedness-from-below (BFB) conditions.

A.2 Unitarity conditions

We consider three matrices:

$$\mathcal{M}_1 = \begin{pmatrix} \lambda_+ + \lambda_4 & \mathrm{Re}\,\bar{\lambda}_+ & -\mathrm{Im}\,\bar{\lambda}_+ & \lambda_- \\ \mathrm{Re}\,\bar{\lambda}_+ & \lambda_3 + \mathrm{Re}\,\lambda_5 & -\mathrm{Im}\,\lambda_5 & \mathrm{Re}\,\bar{\lambda}_- \\ -\mathrm{Im}\,\bar{\lambda}_+ & -\mathrm{Im}\,\lambda_5 & \lambda_3 - \mathrm{Re}\,\lambda_5 & -\mathrm{Im}\,\bar{\lambda}_- \\ \lambda_- & \mathrm{Re}\,\bar{\lambda}_- & -\mathrm{Im}\,\bar{\lambda}_- & \lambda_+ - \lambda_4 \end{pmatrix}, \tag{A.3a}$$

$$\mathcal{M}_2 = \begin{pmatrix} 3\lambda_+ + 2\lambda_3 + \lambda_4 & 3\,\mathrm{Re}\,\bar{\lambda}_+ & -3\,\mathrm{Im}\,\bar{\lambda}_+ & 3\lambda_- \\ 3\,\mathrm{Re}\,\bar{\lambda}_+ & \lambda_3 + 2\lambda_4 + 3\,\mathrm{Re}\,\lambda_5 & -3\,\mathrm{Im}\,\lambda_5 & 3\,\mathrm{Re}\,\bar{\lambda}_- \\ -3\,\mathrm{Im}\,\bar{\lambda}_+ & -3\,\mathrm{Im}\,\lambda_5 & \lambda_3 + 2\lambda_4 - 3\,\mathrm{Re}\,\lambda_5 & -3\,\mathrm{Im}\,\bar{\lambda}_- \\ 3\lambda_- & 3\,\mathrm{Re}\,\bar{\lambda}_- & -3\,\mathrm{Im}\,\bar{\lambda}_- & 3\lambda_+ - 2\lambda_3 - \lambda_4 \end{pmatrix}, \tag{A.3b}$$

$$\mathcal{M}_3 = \begin{pmatrix} \lambda_1 & \lambda_5 & \sqrt{2}\,\lambda_6 \\ \lambda_5^* & \lambda_2 & \sqrt{2}\,\lambda_7^* \\ \sqrt{2}\,\lambda_6^* & \sqrt{2}\,\lambda_7 & \lambda_3 + \lambda_4 \end{pmatrix}. \tag{A.3c}$$

The unitarity conditions are the following [44–46]: the moduli of the eigenvalues of $\mathcal{M}_1$, $\mathcal{M}_2$, and $\mathcal{M}_3$, and also $|\lambda_3 - \lambda_4|$, must be smaller than 8π.

A.3 BFB conditions

We consider the matrix

$$\Lambda_E = \begin{pmatrix} \lambda_+ + \lambda_3 & \mathrm{Re}\,\bar{\lambda}_+ & -\mathrm{Im}\,\bar{\lambda}_+ & \lambda_- \\ -\mathrm{Re}\,\bar{\lambda}_+ & -\lambda_4 - \mathrm{Re}\,\lambda_5 & \mathrm{Im}\,\lambda_5 & -\mathrm{Re}\,\bar{\lambda}_- \\ \mathrm{Im}\,\bar{\lambda}_+ & \mathrm{Im}\,\lambda_5 & -\lambda_4 + \mathrm{Re}\,\lambda_5 & \mathrm{Im}\,\bar{\lambda}_- \\ -\lambda_- & -\mathrm{Re}\,\bar{\lambda}_- & \mathrm{Im}\,\bar{\lambda}_- & -\lambda_+ + \lambda_3 \end{pmatrix}. \tag{A.4}$$

Let Λ_0, Λ_1, Λ_2, and Λ_3 be the eigenvalues of Λ_E. The BFB conditions are the following [47–51]:

1. Λ_0, Λ_1, Λ_2, and Λ_3 are real.

2. The largest eigenvalue, say Λ_0, is positive.

3. The $(1, 1)$ matrix element of the 4×4 matrix

$$(\Lambda_E - \Lambda_1 \times \mathbb{1}_{4\times4}) \times (\Lambda_E - \Lambda_2 \times \mathbb{1}_{4\times4}) \times (\Lambda_E - \Lambda_3 \times \mathbb{1}_{4\times4}) \tag{A.5}$$

   is positive.

A.4 The Higgs basis and the alignment limit

Let $v = 246\,\mathrm{GeV}$ be the vacuum expectation value (VEV). We use the Higgs basis and write $\Phi_{1,2}$ as in (1.4). In order that the doublet Φ_2 has no VEV, the parameter μ_3 must be equal to $-\lambda_6 v^2/2$ [52]. Moreover, $\mu_1 = -\lambda_1 v^2/2$ so that v is the correct value of the VEV [52].

The mass terms of H^+, H, S_3^0, and S_4^0 are given by

$$V = \cdots + m_C^2 H^+ H^- + \frac{1}{2} \left(H, S_3^0, S_4^0 \right) M \begin{pmatrix} H \\ S_3^0 \\ S_4^0 \end{pmatrix}, \qquad (A.6)$$

where $m_C^2 = \mu_2 + v^2 \lambda_3/2$ is the squared mass of the physical charged scalar and [52]

$$M = \begin{pmatrix} v^2 \lambda_1 & v^2 \operatorname{Re} \tilde{\lambda}_6 & -v^2 \operatorname{Im} \tilde{\lambda}_6 \\ v^2 \operatorname{Re} \tilde{\lambda}_6 & m_C^2 + v^2 \left(\lambda_4 + \operatorname{Re} \tilde{\lambda}_5 \right) \big/ 2 & -v^2 \operatorname{Im} \tilde{\lambda}_5 \big/ 2 \\ -v^2 \operatorname{Im} \tilde{\lambda}_6 & -v^2 \operatorname{Im} \tilde{\lambda}_5 \big/ 2 & m_C^2 + v^2 \left(\lambda_4 - \operatorname{Re} \tilde{\lambda}_5 \right) \big/ 2 \end{pmatrix}, \qquad (A.7)$$

where $\tilde{\lambda}_5 := e^{-2i\alpha} \lambda_5$ and $\tilde{\lambda}_6 := e^{-i\alpha} \lambda_6$.

We now assume *alignment*, which means that H has mass $m_H = 125 \,\mathrm{GeV}$ and does not mix with S_3^0 and S_4^0. Clearly, from (A.7), the absence of mixing means $\lambda_6 = 0$, while $m_H^2 = v^2 \lambda_1$, hence

$$\lambda_1 = \left(\frac{125}{246} \right)^2 \approx 0.258. \qquad (A.8)$$

Alignment can be enforced through a $\mathbb{Z}_2$ symmetry $\Phi_2 \to -\Phi_2$ in the so-called inert 2HDM [47, 53–55]. However, that possibility is not suitable for our purposes, because we need all the Yukawa couplings in (1.2) to be nonzero. Therefore, in this letter alignment is just an *ad hoc* assumption. We choose the phase α to offset $\arg \lambda_5$, *viz.* we choose $e^{-2i\alpha} \lambda_5 = \pm |\lambda_5|$. Then, from (A.7) the squared masses of S_3^0 and S_4^0 are

$$M_3^2 = m_C^2 + v^2 \left(\lambda_4 \pm |\lambda_5| \right) \big/ 2 \quad \text{and} \quad M_4^2 = m_C^2 + v^2 \left(\lambda_4 \mp |\lambda_5| \right) \big/ 2, \qquad (A.9)$$

respectively. Their difference is given by $\left| M_3^2 - M_4^2 \right| = v^2 |\lambda_5|$, just as in the scotogenic model [35]. Thus, finding the maximum possible value of $\left| M_3^2 - M_4^2 \right|$ is equivalent to finding the maximum possible value of $|\lambda_5|$, which is determined by the unitarity and BFB conditions.

A.5   Additional conditions

One must guarantee that our assumed vacuum state is indeed the state with the lowest value of V, *viz.* that we are not in the situation where there are two local minima of the potential and we are sitting on the local minimum with the *highest* value of V instead of being at the true vacuum; this undesirable situation has been called 'panic vacuum'. This produces the following condition [49–51, 56]. Let $\zeta \equiv 2m_C^2/v^2$ and let us order the eigenvalues of Λ_E as $\Lambda_0 > \Lambda_1 > \Lambda_2 > \Lambda_3$. Then, either $\zeta > \Lambda_1$ or $\Lambda_2 > \zeta > \Lambda_3$.

There is also a phenomenological condition arising from the oblique parameter T. With alignment [31],

$$T = \frac{1}{16\pi s_w^2 m_W^2} \left[f \left(m_C^2, M_3^2 \right) + f \left(m_C^2, M_4^2 \right) - f \left(M_3^2, M_4^2 \right) \right], \qquad (A.10)$$

where $s_w^2 = 0.22$ is the squared sine of the weak mixing angle, $m_W = 80.4\,\mathrm{GeV}$ is the mass of the $W^\pm$ gauge bosons, and

$$f\left(a,\ b\right) = \begin{cases} \dfrac{a+b}{2} - \dfrac{ab}{a-b}\ln\dfrac{a}{b} & \Leftarrow a \neq b, \\ 0 & \Leftarrow a = b. \end{cases} \tag{A.11}$$

The phenomenological constraint is $T = 0.03 \pm 0.12$ [4].

A.6   The special case $\lambda_1 = \lambda_2,\ \lambda_6 = \lambda_7 = 0$

When $\lambda_6 = \lambda_7 = 0$, i.e. $\bar\lambda_+ = \bar\lambda_- = 0$, the matrices $\mathcal{M}_{1,2,3}$ and Λ_E decompose as 2×2 matrices, their eigenvalues are easy to compute, and the unitarity and BFB conditions become much simpler [17]. With the additional condition $\lambda_1 = \lambda_2$, they are

$$|\lambda_3 \pm \lambda_4| < 8\pi, \tag{A.12a}$$

$$|\lambda_3 \pm |\lambda_5|| < 8\pi, \tag{A.12b}$$

$$|\lambda_3 + 2\lambda_4 \pm 3|\lambda_5|| < 8\pi, \tag{A.12c}$$

$$|\lambda_1 \pm |\lambda_5|| < 8\pi, \tag{A.12d}$$

$$|\lambda_1 \pm \lambda_4| < 8\pi, \tag{A.12e}$$

$$|2\lambda_3 + \lambda_4 \pm 3\lambda_1| < 8\pi, \tag{A.12f}$$

$$\lambda_1 > 0, \tag{A.12g}$$

$$\lambda_3 > -\lambda_1, \tag{A.12h}$$

$$|\lambda_5| < \lambda_1 + \lambda_3 + \lambda_4. \tag{A.12i}$$

Notice that in this case

$$\Lambda_0 = \lambda_3 + \lambda_1 \tag{A.13}$$

while Λ_1, Λ_2, and Λ_3 are some permutation of

$$\lambda_3 - \lambda_1, \quad -\lambda_4 + |\lambda_5|, \quad \text{and} \ -\lambda_4 - |\lambda_5|. \tag{A.14}$$

A.7   A solution

With λ_1 given by (A.8), there is a solution to (A.12):

$$\lambda_3 = \frac{16\pi}{3} - 2\lambda_1 - \epsilon, \qquad \lambda_4 = -\frac{8\pi}{3} + \lambda_1 + \epsilon, \qquad |\lambda_5| = \frac{8\pi}{3} - \epsilon, \tag{A.15}$$

where

$$0 < \epsilon < \frac{8\pi}{3}. \tag{A.16}$$

With this solution we learn that $|\lambda_5|$ may be as high as 8.377, and therefore $|M_3^2 - M_4^2| \lesssim 5.07 \times 10^5\,\mathrm{GeV}^2$. For instance, with $(M_3 + M_4)/2 = 1\,\mathrm{TeV}$ one has $|M_3 - M_4| \lesssim 253\,\mathrm{GeV}$.

With (A.15),

$$\left\{M_3^2,\ M_4^2\right\} = \left\{m_C^2 + v^2\,\frac{\lambda_1}{2},\ m_C^2 + v^2\left(-\frac{8\pi}{3} + \frac{\lambda_1}{2} + \epsilon\right)\right\}. \tag{A.17}$$

We are interested in the situation where ϵ is rather small, so that $|\lambda_5|$ is not very far from $8\pi/3$. When ϵ is small, m_C^2 lies in between the M_3^2 and M_4^2 given in (A.17), but it is very close to one of them because λ_1 is so small. Then, T is negative but very small, automatically satisfying the phenomenological constraint on that parameter.

With (A.15) one has

$$\{\Lambda_1, \ \Lambda_2\} = \left\{ \frac{16\pi}{3} - 3\lambda_1 - \epsilon, \ \frac{16\pi}{3} - \lambda_1 - 2\epsilon \right\}. \tag{A.18}$$

Therefore, if we choose

$$m_C^2 \geq v^2 \left(\frac{8\pi}{3} - \frac{\lambda_1}{2} \right), \tag{A.19}$$

we avoid the undesirable situation of panic vacuum. Thus, we must have $m_C \gtrsim 707\,\text{GeV}$. This lower bound on m_C coincides with an analogous bound obtained in a recent phenomenological analysis [41].

Our solution (A.15) explicitly demonstrates that $\left| M_3^2 - M_4^2 \right|$ may reach $v^2 \, (8\pi/3)$ without violating the unitarity and BFB conditions and with a very small oblique parameter T. Moreover, the inequality (A.19) provides a way to choose the mass of the physical charged scalar such as to evade panic vacuum.

References

[1] SUPER-KAMIOKANDE collaboration, *Evidence for oscillation of atmospheric neutrinos*, *Phys. Rev. Lett.* **81** (1998) 1562 [hep-ex/9807003] [INSPIRE].

[2] SNO collaboration, *Measurement of the rate of $\nu_e + d \rightarrow p + p + e^-$ interactions produced by ^8B solar neutrinos at the Sudbury Neutrino Observatory*, *Phys. Rev. Lett.* **87** (2001) 071301 [nucl-ex/0106015] [INSPIRE].

[3] SNO collaboration, *Combined Analysis of all Three Phases of Solar Neutrino Data from the Sudbury Neutrino Observatory*, *Phys. Rev. C* **88** (2013) 025501 [arXiv:1109.0763] [INSPIRE].

[4] PARTICLE DATA GROUP collaboration, *Review of Particle Physics*, *Prog. Theor. Exp. Phys.* **2020** (2020) 083C01 [INSPIRE].

[5] A. Blondel et al., *Research Proposal for an Experiment to Search for the Decay $\mu \rightarrow eee$*, arXiv:1301.6113 [INSPIRE].

[6] T. Aushev et al., *Physics at Super B Factory*, arXiv:1002.5012 [INSPIRE].

[7] A. Cerri et al., *Report from Working Group 4*: Opportunities in Flavour Physics at the HL-LHC and HE-LHC, *CERN Yellow Rep. Monogr.* **7** (2019) 867 [arXiv:1812.07638] [INSPIRE].

[8] P. Azzi et al., *Report from Working Group 1*: Standard Model Physics at the HL-LHC and HE-LHC, *CERN Yellow Rep. Monogr.* **7** (2019) 1 [arXiv:1902.04070] [INSPIRE].

[9] BELLE-II collaboration, *The Belle II Physics Book*, *PTEP* **2019** (2019) 123C01 [*Erratum ibid.* **2020** (2020) 029201] [`arXiv:1808.10567`] [INSPIRE].

[10] A. Vicente, *Higgs lepton flavor violating decays in Two Higgs Doublet Models*, *Front. in Phys.* **7** (2019) 174 [`arXiv:1908.07759`] [INSPIRE].

[11] S.T. Petcov, *The Processes $\mu \to e + \gamma, \mu \to e + \overline{e}, \nu' \to \nu + \gamma$ in the Weinberg-Salam Model with Neutrino Mixing*, *Sov. J. Nucl. Phys.* **25** (1977) 340 [*Erratum ibid.* **25** (1977) 698] [*Erratum ibid.* **25** (1977) 1336] [INSPIRE].

[12] S.M. Bilenky and S.T. Petcov, *Massive Neutrinos and Neutrino Oscillations*, *Rev. Mod. Phys.* **59** (1987) 671 [*Erratum ibid.* **60** (1988) 575] [*Erratum ibid.* **61** (1989) 169] [INSPIRE].

[13] G. Hernández-Tomé, G. López Castro and P. Roig, *Flavor violating leptonic decays of τ and μ leptons in the Standard Model with massive neutrinos*, *Eur. Phys. J. C* **79** (2019) 84 [*Erratum ibid.* **80** (2020) 438] [`arXiv:1807.06050`] [INSPIRE].

[14] P. Blackstone, M. Fael and E. Passemar, *$\tau \to \mu\mu\mu$ at a rate of one out of 10^{14} tau decays?*, *Eur. Phys. J. C* **80** (2020) 506 [`arXiv:1912.09862`] [INSPIRE].

[15] W. Grimus and L. Lavoura, *Soft lepton flavor violation in a multi Higgs doublet seesaw model*, *Phys. Rev. D* **66** (2002) 014016 [`hep-ph/0204070`] [INSPIRE].

[16] E.H. Aeikens, W. Grimus and L. Lavoura, *Charged-lepton decays from soft flavour violation*, *Phys. Lett. B* **768** (2017) 365 [`arXiv:1612.00724`] [INSPIRE].

[17] G.C. Branco, P.M. Ferreira, L. Lavoura, M.N. Rebelo, M. Sher and J.P. Silva, *Theory and phenomenology of two-Higgs-doublet models*, *Phys. Rept.* **516** (2012) 1 [`arXiv:1106.0034`] [INSPIRE].

[18] I.P. Ivanov, *Building and testing models with extended Higgs sectors*, *Prog. Part. Nucl. Phys.* **95** (2017) 160 [`arXiv:1702.03776`] [INSPIRE].

[19] P. Minkowski, *$\mu \to e\gamma$ at a Rate of One Out of 10^9 Muon Decays?*, *Phys. Lett. B* **67** (1977) 421 [INSPIRE].

[20] T. Yanagida, *Horizontal gauge symmetry and masses of neutrinos*, in *Proceedings of the workshop on unified theory and baryon number in the universe*, Tsukuba, Japan (1979), O. Sawata and A. Sugamoto eds., KEK report 79-18, Tsukuba (1979) [INSPIRE].

[21] S.L. Glashow, *The future of elementary particle physics*, in *Quarks and leptons, proceedings of the advanced study institute*, Cargèse, Corsica (1979), M. Lévy et al. eds., Plenum, New York (1980) [INSPIRE].

[22] M. Gell-Mann, P. Ramond and R. Slansky, *Complex spinors and unified theories*, in *Supergravity*, D.Z. Freedman and F. van Nieuwenhuizen eds., North Holland, Amsterdam (1979) [INSPIRE].

[23] R.N. Mohapatra and G. Senjanović, *Neutrino Mass and Spontaneous Parity Nonconservation*, *Phys. Rev. Lett.* **44** (1980) 912 [INSPIRE].

[24] L. Lavoura and W. Grimus, *Seesaw model with softly broken $L_e - L_\mu - L_\tau$*, *JHEP* **09** (2000) 007 [`hep-ph/0008020`] [INSPIRE].

[25] T.A. Chowdhury and S. Nasri, *Charged Lepton Flavor Violation in a class of Radiative Neutrino Mass Generation Models*, *Phys. Rev. D* **97** (2018) 075042 [`arXiv:1801.07199`] [INSPIRE].

[26] W. Grimus and L. Lavoura, *One-loop corrections to the seesaw mechanism in the multi-Higgs-doublet standard model*, *Phys. Lett. B* **546** (2002) 86 [hep-ph/0207229] [INSPIRE].

[27] W. Grimus and H. Neufeld, *Radiative Neutrino Masses in an* SU(2) × U(1) *Model*, *Nucl. Phys. B* **325** (1989) 18 [INSPIRE].

[28] A. Ibarra and C. Simonetto, *Understanding neutrino properties from decoupling right-handed neutrinos and extra Higgs doublets*, *JHEP* **11** (2011) 022 [arXiv:1107.2386] [INSPIRE].

[29] D. Jurčiukonis, T. Gajdosik and A. Juodagalvis, *Seesaw neutrinos with one right-handed singlet field and a second Higgs doublet*, *JHEP* **11** (2019) 146 [arXiv:1909.00752] [INSPIRE].

[30] D. Aristizabal Sierra and C.E. Yaguna, *On the importance of the 1-loop finite corrections to seesaw neutrino masses*, *JHEP* **08** (2011) 013 [arXiv:1106.3587] [INSPIRE].

[31] W. Grimus, L. Lavoura, O.M. Ogreid and P. Osland, *A Precision constraint on multi-Higgs-doublet models*, *J. Phys. G* **35** (2008) 075001 [arXiv:0711.4022] [INSPIRE].

[32] ATLAS and CMS collaborations, *Combined Measurement of the Higgs Boson Mass in pp Collisions at $\sqrt{s} = 7$ and 8 TeV with the ATLAS and CMS Experiments*, *Phys. Rev. Lett.* **114** (2015) 191803 [arXiv:1503.07589] [INSPIRE].

[33] ATLAS and CMS collaborations, *Measurements of the Higgs boson production and decay rates and constraints on its couplings from a combined ATLAS and CMS analysis of the LHC pp collision data at $\sqrt{s} = 7$ and 8 TeV*, *JHEP* **08** (2016) 045 [arXiv:1606.02266] [INSPIRE].

[34] Y. Nir, *The three jewels in the crown of the LHC*, *CERN Cour.* **60** (2020) 41 [arXiv:2010.13126] [INSPIRE].

[35] E. Ma, *Verifiable radiative seesaw mechanism of neutrino mass and dark matter*, *Phys. Rev. D* **73** (2006) 077301 [hep-ph/0601225] [INSPIRE].

[36] I. Esteban, M.C. Gonzalez-Garcia, A. Hernandez-Cabezudo, M. Maltoni and T. Schwetz, *Global analysis of three-flavour neutrino oscillations: synergies and tensions in the determination of θ_{23}, δ_{CP}, and the mass ordering*, *JHEP* **01** (2019) 106 [arXiv:1811.05487] [INSPIRE].

[37] F. Capozzi, E. Di Valentino, E. Lisi, A. Marrone, A. Melchiorri and A. Palazzo, *Global constraints on absolute neutrino masses and their ordering*, *Phys. Rev. D* **95** (2017) 096014 [*Addendum ibid.* **101** (2020) 116013] [arXiv:2003.08511] [INSPIRE].

[38] P.F. de Salas et al., *2020 Global reassessment of the neutrino oscillation picture*, arXiv:2006.11237 [INSPIRE].

[39] I. Esteban, M.C. Gonzalez-Garcia, M. Maltoni, T. Schwetz and A. Zhou, *The fate of hints: updated global analysis of three-flavor neutrino oscillations*, *JHEP* **09** (2020) 178 [arXiv:2007.14792] [INSPIRE].

[40] PLANCK collaboration, *Planck 2018 results. I. Overview and the cosmological legacy of Planck*, *Astron. Astrophys.* **641** (2020) A1 [arXiv:1807.06205] [INSPIRE].

[41] D. Chowdhury and O. Eberhardt, *Update of Global Two-Higgs-Doublet Model Fits*, *JHEP* **05** (2018) 161 [arXiv:1711.02095] [INSPIRE].

[42] D. Jurčiukonis and L. Lavoura, *The three- and four-Higgs couplings in the general two-Higgs-doublet model*, *JHEP* **12** (2018) 004 [arXiv:1807.04244] [INSPIRE].

[43] H. Novales-Sánchez, M. Salinas and J.J. Toscano, *About heavy neutrinos: Lepton-flavor violation in decays of charged leptons*, *J. Phys. G* **45** (2018) 095004 [`arXiv:1710.08474`] [ɪɴSPIRE].

[44] S. Kanemura, T. Kubota and E. Takasugi, *Lee-Quigg-Thacker bounds for Higgs boson masses in a two doublet model*, *Phys. Lett. B* **313** (1993) 155 [`hep-ph/9303263`] [ɪɴSPIRE].

[45] A.G. Akeroyd, A. Arhrib and E.-M. Naimi, *Note on tree level unitarity in the general two Higgs doublet model*, *Phys. Lett. B* **490** (2000) 119 [`hep-ph/0006035`] [ɪɴSPIRE].

[46] I.F. Ginzburg and I.P. Ivanov, *Tree-level unitarity constraints in the most general 2HDM*, *Phys. Rev. D* **72** (2005) 115010 [`hep-ph/0508020`] [ɪɴSPIRE].

[47] N.G. Deshpande and E. Ma, *Pattern of Symmetry Breaking with Two Higgs Doublets*, *Phys. Rev. D* **18** (1978) 2574 [ɪɴSPIRE].

[48] M. Maniatis, A. von Manteuffel, O. Nachtmann and F. Nagel, *Stability and symmetry breaking in the general two-Higgs-doublet model*, *Eur. Phys. J. C* **48** (2006) 805 [`hep-ph/0605184`] [ɪɴSPIRE].

[49] I.P. Ivanov, *Minkowski space structure of the Higgs potential in 2HDM*, *Phys. Rev. D* **75** (2007) 035001 [*Erratum ibid.* **76** (2007) 039902] [`hep-ph/0609018`] [ɪɴSPIRE].

[50] I.P. Ivanov, *Minkowski space structure of the Higgs potential in 2HDM. II. Minima, symmetries, and topology*, *Phys. Rev. D* **77** (2008) 015017 [`arXiv:0710.3490`] [ɪɴSPIRE].

[51] I.P. Ivanov and J.P. Silva, *Tree-level metastability bounds for the most general two Higgs doublet model*, *Phys. Rev. D* **92** (2015) 055017 [`arXiv:1507.05100`] [ɪɴSPIRE].

[52] L. Lavoura and J.P. Silva, *Fundamental CP-violating quantities in a* SU(2) × U(1) *model with many Higgs doublets*, *Phys. Rev. D* **50** (1994) 4619 [`hep-ph/9404276`] [ɪɴSPIRE].

[53] R. Barbieri, L.J. Hall and V.S. Rychkov, *Improved naturalness with a heavy Higgs: An Alternative road to LHC physics*, *Phys. Rev. D* **74** (2006) 015007 [`hep-ph/0603188`] [ɪɴSPIRE].

[54] Q.-H. Cao, E. Ma and G. Rajasekaran, *Observing the Dark Scalar Doublet and its Impact on the Standard-Model Higgs Boson at Colliders*, *Phys. Rev. D* **76** (2007) 095011 [`arXiv:0708.2939`] [ɪɴSPIRE].

[55] L. Lopez Honorez, E. Nezri, J.F. Oliver and M.H.G. Tytgat, *The Inert Doublet Model: An Archetype for Dark Matter*, *JCAP* **02** (2007) 028 [`hep-ph/0612275`] [ɪɴSPIRE].

[56] A. Barroso, P.M. Ferreira, I.P. Ivanov, R. Santos and J.P. Silva, *Evading death by vacuum*, *Eur. Phys. J. C* **73** (2013) 2537 [`arXiv:1211.6119`] [ɪɴSPIRE].